*Journal of Computational and Applied Mechanics, Vol. 10., No. 2., (2015), pp. 231–268*

# ANALYSIS OF STEADY WEAR PROCESSES FOR PERIODIC SLIDING

István Páczelt
Institute of Applied Mechanics, University of Miskolc
H-3515 Miskolc, Miskolc–Egyetemváros, Hungary
mechpacz@uni-miskolc.hu

Zenon Mróz
Institute of Fundamental Technological Research, A. Pawińskiego 5B, 02-106 Warsaw, Poland
zmroz@ippt.pl

Attila Baksa
Institute of Applied Mechanics, University of Miskolc
H-3515 Miskolc, Miskolc–Egyetemváros, Hungary
attila.baksa@uni-miskolc.hu

[Received: June 14, 2015, Accepted: September 2, 2015]

*Dedicated to Professor Barna Szabó on the occasion of his eightieth birthday and to Professor Imre Kozák on the occasion of his eighty-fifth birthday*

**Abstract.** The relative sliding motion of two elastic bodies in contact induces the wear process and contact shape evolution. The transient process at the constant relative velocity between the bodies tends to a steady state occurring at fixed contact stress and strain distribution. This state corresponds to a minimum of the wear dissipation power. The optimality conditions of the functional provide a contact stress distribution and a wear rate compatible with the rigid body punch motion. The present paper is devoted to the analysis of wear processes occurring for periodic sliding of contacting bodies, assuming cyclic steady state conditions for mechanical fields. From the condition of the rigid body wear velocity a formula for summarized contact pressure in the periodic steady state is derived. The optimization problem is formulated for calculation of the contact surface shape induced by wear in the steady periodic state.

*Mathematical Subject Classification:*
*Keywords*: steady wear process, periodic sliding, unilateral contact, p-version of finite element method, shape optimization

## 1. Introduction

The wear process on the frictional interface of two bodies in a relative sliding motion induces shape evolution. In many practical industrial applications it is very important to predict the form of wear shape and contact stresses. Usually the simulation of the

©2015 Miskolc University Press

contact shape evolution is performed by numerical integration of the modified Archard wear rule expressed in terms of the relative slip velocity and contact pressure.

For cases of monotonic sliding motion the minimization of the wear dissipation power provides the contact pressure distribution and rigid body wear velocities directly without time integration of the wear rule until the steady state is reached, cf. [1, 2, 3, 4]. (The steady state is reached when the contact stress is fixed with respect to the moving contact domain and the rigid body wear velocity is constant in time.) The quasi-steady wear state is reached for the stress distribution dependent on a slowly varying contact domain $S_c(t)$. It is important that in general contact conditions the vector of wear rate is not normal to the contact surface and has a tangential component [1]. A fundamental assumption was introduced, namely, *in the steady state the wear rate vector is collinear with the rigid body wear velocity of a sliding body allowed by boundary constraints.*

In [1] a new idea of the wear rate vector and new form of the wear dissipation power was presented. This new principle was applied in the analysis of the steady wear states in disk and drum brakes.

Next, this approach was extended in [2] by the authors of previous analysis to specification of steady-state contact shapes with coupled wear and thermal distortion effects taken into account. The wear rule was assumed as a non-linear relation of wear rate to shear stress and relative sliding velocity. The analysis of wear of disks and drum brakes was presented with the thermal distortion effect.

In [3] an improved numerical analysis of the thermo-elastic contact coupled with wear process was developed. The coupled thermo-mechanical problem was numerically treated by applying the operator split technique. For larger values of relative sliding velocities and moving frictional heat fluxes the thermal analysis requires application of the upwind technique. Neglecting temperature dependence of material parameters, it was concluded that the contact pressure distribution in the steady-state is not affected by temperature field, but the contact surface shape reached in the wear process strongly depends on the thermal distortion. A brake system with different shoes support was investigated, deriving the contact pressure distribution also for the steady wear state.

In [4] the numerical analysis of coupled thermo-elastic steady wear regimes was presented: wear analysis of a punch translating on an elastic strip and wear induced by a rotating punch on a toroidal surface. The wear and friction parameters were assumed as fixed or temperature dependent. The incremental procedure for temperature dependent parameters was established. Three transverse friction models were discussed accounting for the effect of wear debris motion. It was demonstrated, that the contact pressure distribution depends only on the transformed wear velocities, friction coefficient and wear parameter $b$, and is not dependent on relative velocity and wear parameter $\tilde{\beta}_i$ (see (1)). The contact conformity condition was defined. In the cases of wear of punch and wear of two bodies the contact pressure distribution in the steady state is governed by the relative rigid body motion induced by wear.

On the other hand, when only wear of the substrate takes place, the contact pressure distribution is specified from the contact conformity condition and depends on the elastic moduli of contacting bodies. In the literature there are numerous works dealing with fretting problems, when in the contact domain both adhesion and slip sub-regions can develop, [5, 6, 7, 8, 9]. Periodic contact sliding was treated in some papers, cf. [10, 11].

The extension of variational method is presented for the case of multi-zone contact problems for steady wear states in [12] which both transient and steady states have been analyzed.

Paper [13] was aimed at extending the results of previous analyses [1, 2, 3, 4] of steady state conditions to cases of periodic sliding of contacting bodies, assuming the existence of cyclic steady state conditions. In the time integration it was assumed that contact pressure distribution is fixed during the semi-cycle and varies discontinuously during sliding reversal in consecutive semi-cycles. The $p$-version of the finite element method is well suited for solving the contact problems with high accuracy, using the blending technique for approximation of the shape. Wear prediction was made in the brake system by using the averaging technique of results from monotonic motions. The contact pressure distribution has been derived in the discretized form for 3 cases using the Green functions. *Case 1*: wear of both punch and substrate, *Case 2*: wear of substrate only, *Case 3*: wear of punch only. In particular, the body $B_1$ can be regarded as a punch translating and rotating relative to the substrate.

Several classes of wear problems can be distinguished and discussed for specified loading and support conditions for two bodies in the relative sliding motion. *Class 1*: The contact zone $S_c$ is fixed on one of the sliding bodies (like a punch) and translates on the surface of the other body (substrate). The rigid body wear velocity is compatible with the specified boundary conditions. The steady state condition is reached when the contact pressure distribution corresponds to the wear rate proportional to the rigid body velocity [2, 3]. The relative velocity between the bodies is constant in time. *Class 2*: Similarly to Class 1, the contact zone $S_c$ is fixed but the wear process occurs for periodic sliding motion. *Class 3*: Similarly to Class 1, the relative velocity is constant, but the load is periodic in time. Class 4: Similarly to Class 2, the contact zone is fixed, but the wear process reaches the steady state for periodic load and periodic sliding motion (for instance in the braking process). In the case of *Class 1*, from minimization of the wear dissipation power it is easy to derive the formulae for contact pressure distribution [2, 3]. Paper [6] presents the analysis of wear for the case of periodic sliding of contacting bodies, assuming cyclic steady state conditions and taking into the heat generation at the contact surface. In particular, the body $B_1$ can be regarded as a punch translating and rotating relative to the substrate $B_2$.

It is assumed that strains are small and the materials of the contacting bodies are linearly elastic. In discretization of the contacting bodies for the displacement and temperature determination, the $p$-version of finite elements was used [13, 14], assuring fast convergence of the numerical process and providing a high level accuracy of geometry for shape optimization.

The specific examples are related to the analysis of punch wear induced by reciprocal sliding along a rectilinear path on an elastic strip. The external loads acting on the punch are not symmetric. Specifying the steady state contact pressure distributions for an arbitrarily constrained punch, it is noted that the pressure at one contact edge vanishes, and the maximal pressure is reached at the other edge. It was shown that by summarizing pressure values for consecutive semi-cycles, a resulting distribution is obtained that corresponds to the rigid body displacement of the punch. The analysis of the same example taking heat generation into account demonstrates that the thermal distortion affects essentially the contact shape and the transient contact pressure distribution [15]. However, it was shown that in the steady wear state for reciprocal sliding, the contact pressure reaches the same distribution as that obtained for the case of neglect of heat generation, but the steady state contact shapes are different.

In the case of periodic sliding motion, the steady state cyclic solution should be specified and the averaged pressure in one cycle and the averaged wear velocity can be determined from the averaged wear dissipation in one cycle. In our investigation between the bodies it was assumed that the stick zone no longer exists and the whole contact zone undergoes sliding. The tangential stress can then be directly calculated from the contact pressure and the coefficient of friction.

## 2. Wear rule and wear rate vector

The modified Archard wear rule [1] specifies the wear rate $\dot{w}_{i,n}$ of the $i$-th body in the normal contact direction. Following previous work [1, 2] it is assumed that

$$\dot{w}_{i,n} = \beta_i(\tau_n)^{b_i}\|\dot{\boldsymbol{u}}_\tau\|^{a_i} = \beta_i(\mu\, p_n)^{b_i}\|\dot{\boldsymbol{u}}_\tau\|^{a_i} = \beta_i(\mu\, p_n)^{b_i} v_r^{a_i} = \tilde{\beta}_i p_n^{b_i} v_r^{a_i}, \quad i = 1,2 \quad (1)$$

where $\mu$ is the friction coefficient, $\beta_i$, $a_i$, $b_i$ are the wear parameters, $\tilde{\beta}_i = \beta_i \mu^{b_i}$, $v_r = \|\dot{\boldsymbol{u}}_\tau\|$ is the relative tangential velocity between the bodies, constrained by the boundary conditions.

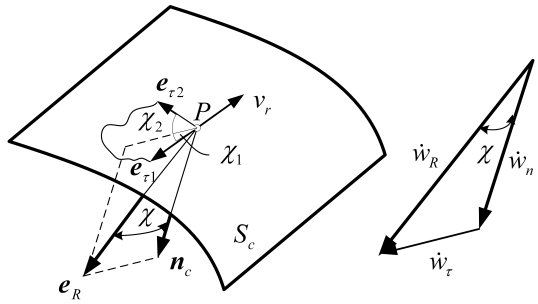


Figure 1. Reference frame and wear rate vectors on the contact surface $S_c$. Coaxiality rule of $\dot{\boldsymbol{w}}_R$ and $\boldsymbol{e}_R$.

The shear stress at the contact surface is expressed in terms of the contact pressure $p_n$ by the Coulomb friction law $\tau_n = \mu p_n$. In general contact conditions the wear rate vector $\dot{\boldsymbol{w}}_i$ is not normal to the contact surface and results from the constraints imposed on the rigid body motion of punch $B_1$. Introducing the local reference triad

$\boldsymbol{e}_{\tau 1}$, $\boldsymbol{e}_{\tau 2}$, $\boldsymbol{n}_c$ on the contact surface $S_c$ (see Figure 1), where $\boldsymbol{n}_c$ is the unit normal vector, directed into body $B_2$, $\boldsymbol{n}_i$ is the unit surface normal of the $i$-th body, $\boldsymbol{e}_{\tau_1}$ is the unit tangent vector coaxial with the sliding velocity and $\boldsymbol{e}_{\tau_2}$ is the transverse unit vector, the wear rate vectors of bodies $B_1$ and $B_2$ are

$$\dot{\boldsymbol{w}}_1 = -\dot{w}_{1,n}\,\boldsymbol{n}_c + \dot{w}_{1,\tau 1}\,\boldsymbol{e}_{\tau 1} + \dot{w}_{1,\tau 2}\,\boldsymbol{e}_{\tau 2}\,, \quad \dot{\boldsymbol{w}}_2 = \dot{w}_{2,n}\,\boldsymbol{n}_c - \dot{w}_{2,\tau 1}\,\boldsymbol{e}_{\tau 1} - \dot{w}_{2,\tau 2}\,\boldsymbol{e}_{\tau 2}\,. \tag{2}$$

The contact traction on $S_c$ can be expressed as follows [3]

$$\boldsymbol{t}^c = \boldsymbol{t}_1^c = -\boldsymbol{t}_2^c = -p_n^{\pm}\boldsymbol{\rho}_c^{\pm}\,, \quad \boldsymbol{\rho}_c^{\pm} = \boldsymbol{n}_c \pm \mu\,\boldsymbol{e}_{\tau 1} + \mu_d\,\boldsymbol{e}_{\tau 2} \tag{3}$$

where $\boldsymbol{\rho}_c^{\pm}$ specifies the orientation and magnitude of traction $\boldsymbol{t}^c$ with reference to the contact pressure $p_n$ and $\mu_d$ is the transverse friction coefficient. The sign + in (2) corresponds to the case when the relative tangential velocity is $\dot{\boldsymbol{u}}_\tau = \dot{\boldsymbol{u}}_\tau^{(2)} - \dot{\boldsymbol{u}}_\tau^{(1)} = -\|\dot{\boldsymbol{u}}_\tau\|\,\boldsymbol{e}_{\tau 1} = -v_r\boldsymbol{e}_{\tau 1}$ with the corresponding shear stress acting on the body $B_1$ along $-\boldsymbol{e}_{\tau 1}$. The fundamental coaxiality rule was stated by Páczelt and Mróz [1, 2, 3, 4], namely: in the steady state the wear rate vector $\dot{\boldsymbol{w}}_R$ is collinear with the rigid body wear velocity vector $\dot{\boldsymbol{\lambda}}_R$, thus

$$\dot{\boldsymbol{w}}_R = \dot{w}_R\,\boldsymbol{e}_R\,, \quad \boldsymbol{e}_R = \frac{\dot{\boldsymbol{\lambda}}_R}{\left\|\dot{\boldsymbol{\lambda}}_R\right\|} = \frac{\dot{\boldsymbol{\lambda}}_F + \dot{\boldsymbol{\lambda}}_M \times \Delta\boldsymbol{r}}{\left\|\dot{\boldsymbol{\lambda}}_F + \dot{\boldsymbol{\lambda}}_M \times \Delta\boldsymbol{r}\right\|}\,, \tag{4}$$

where $\Delta\boldsymbol{r}$ is the position vector. The coaxiality rule is illustrated in Figure 1. The normal and tangential wear rate components now are

$$\dot{w}_n = \dot{w}_R \cos\chi\,, \quad \dot{w}_\tau = \dot{w}_R\,\sin\chi = \dot{w}_n\,\tan\chi \tag{5}$$

where $\chi$ is the angle between $\boldsymbol{n}_c$ and $\boldsymbol{e}_R$ . The wear rate components in the tangential directions are

$$\dot{w}_{\tau 1} = w_R\,\sin\chi\,\cos\chi_1\,, \quad \dot{w}_{\tau 2} = w_R\,\sin\chi\,\sin\chi_1 \tag{6}$$

where the angle $\chi_1$ is formed between the projection of $\dot{\boldsymbol{w}}_R$ on $S_c$ and $\boldsymbol{e}_{\tau,1}$ as shown in Figure 1. Let us note that the sliding velocity $v_r = \|\dot{\boldsymbol{u}}_\tau\|$ is specified from the boundary conditions and the wear velocity vectors $\dot{\boldsymbol{\lambda}}_F$ and $\dot{\boldsymbol{\lambda}}_M$ should be determined from the solution of a specific problem. In the analysis of sliding wear problems the elastic term of relative sliding velocity is usually neglected.

## 3. Steady state conditions for monotonic motion

It has been shown in [1, 2] that the steady state conditions for monotonic motion can be obtained from minimization of the wear dissipation power subject to equilibrium constraints for body $B_1$. The wear dissipation power for the case of wear of two bodies equals

$$D_w = \sum_{i=1}^{2}\left(\int_{S_c}(\boldsymbol{t}_i^c \cdot \dot{\boldsymbol{w}}_i)\,\mathrm{d}S\right) = \sum_{i=1}^{2} C_i\,. \tag{7}$$

The global equilibrium conditions for the body $B_1$ can be expressed as follows

$$\begin{aligned} \boldsymbol{f} &= -\int_{S_c} \boldsymbol{\rho}_c^{\pm}\, p_n^{\pm}\, \mathrm{d}S + \boldsymbol{f}_0 = \boldsymbol{0} \\ \boldsymbol{m} &= -\int_{S_c} \Delta \boldsymbol{r} \times \boldsymbol{\rho}_c^{\pm}\, p_n^{\pm}\, \mathrm{d}S + \boldsymbol{m}_0 = \boldsymbol{0} \end{aligned} \tag{8}$$

where $\boldsymbol{f}_0$ and $\boldsymbol{m}_0$ denote the resultant force and moment acting on the body $B_1$ . The formula for contact pressure at steady wear state can be found in papers [1, 2, 4] and for multi-contact zone cases the contact pressure's formula can be found in [12].

## 4. Wear dissipation in periodic motion and summed pressure in periodic steady wear state

In this section we shall analyze the wear process induced by the reciprocal strip translation. It is assumed that only the punch undergoes wear (see Figure 2), that is in our case $\tilde{\beta}_1 \neq 0, \quad \tilde{\beta}_2 = 0$.

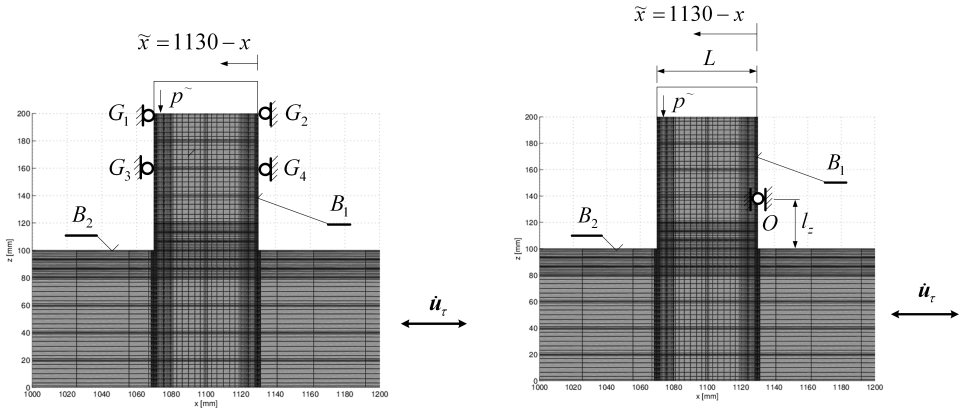


a) b)

Figure 2. Periodic sliding on the contact interface between punch and strip. The number of finite elements in body 1 along the $x$ direction is 8, and in vertical $z$ direction is 7. The lines are drown through the Lobatto integral coordinates.

In the analysis the contact pressure distribution is assumed as fixed during semi-cycle and varies discontinuously during sliding reversal in consecutive semi-cycles. The temperature distribution varies continuously during each cycle period [15]. The coupled thermo-mechanical problem was solved by the operator split technique [16]. The wear effect is calculated incrementally by applying the Archard type wear rule (1). The wear is accumulated at the end of the half period of motion, so the contact pressure is fixed (at the iteration level), and the transient heat conduction problem is next solved for the given temperature field at the beginning of the half period.

The steady state contact pressure distribution in the wear process induced by periodic sliding does not depend on the value of wear factor $\tilde{\beta}_1$ nor generated temperature field, but the wear induced contact surface shape is strongly affected.

During the steady periodic response the wear increment accumulated during one cycle should be compatible at each point $x \in S_c$ with the rigid body punch motion.

The wear dissipation work for periodic motion is

$$E_w = \frac{1}{2}\sum_{i=1}^{2}\int_0^{T_*/2}\left(\int_{S_c^{(i)}} (\boldsymbol{t}_i^{c+}\cdot\dot{\boldsymbol{w}}_i^{+})\,\mathrm{d}S\right)\mathrm{d}\tau + \frac{1}{2}\sum_{i=1}^{2}\int_{T_*/2}^{T_*}\left(\int_{S_c^{(i)}} (\boldsymbol{t}_i^{c-}\cdot\dot{\boldsymbol{w}}_i^{-})\,\mathrm{d}S\right)\mathrm{d}\tau \tag{9}$$

where $\boldsymbol{t}_i^{c+}$, $\boldsymbol{t}_i^{c-}$ is the contact traction vector and $\dot{\boldsymbol{w}}_i^{+}$, $\dot{\boldsymbol{w}}_i^{-}$ is the wear velocity of the i-th body in the progressive and reciprocal motion direction, $T_*$ is the period of sliding motion, $T_* = 2\pi/\omega$.

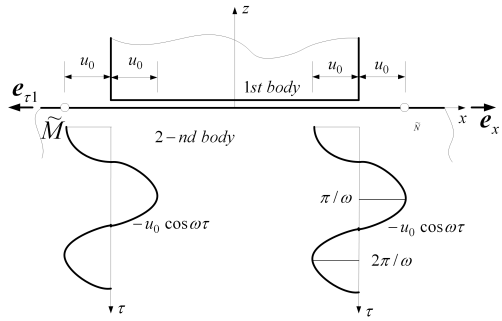


$$\boldsymbol{u}_\tau = -u_0\cos\omega\tau\,\boldsymbol{e}_x = u_0\cos\omega\tau\,\boldsymbol{e}_{\tau 1}$$

Figure 3. The wear process occurring on the contact interface between punch and strip translating with the relative velocity $v_r = u_0\,\omega\,\sin\omega\tau$, $\dot{\boldsymbol{u}}_\tau = -v_r\,\boldsymbol{e}_{\tau 1}$. The segment $\tilde{M}\tilde{N}$ of the substrate takes part in the wear process.

In our case the tangential velocity of body 2 is (see Figure 3):

$$\dot{\boldsymbol{u}}_\tau = \dot{\boldsymbol{u}}_\tau^{(2)} - \dot{\boldsymbol{u}}_\tau^{(1)} = u_0\,\omega\sin\omega\tau\,\boldsymbol{e}_x = -u_0\,\omega\sin\omega\tau\,\boldsymbol{e}_{\tau 1} = -v_r\,\boldsymbol{e}_{\tau 1} \tag{10}$$

with the corresponding shear stress acting on the body $B_1$ along $-\boldsymbol{e}_{\tau 1}$. The integral of the relative velocity between the bodies is

$$\int_0^{T_*/2} v_r\mathrm{d}\tau = \int_{T_*/2}^{T_*} v_r\mathrm{d}\tau = 2u_0\,. \tag{11}$$

In view of the wear rule (1) the wear dissipation for the punch of Figure 2 is

$$E_w = \frac{1}{2}\sum_{i=1}^{1}\int_0^{T_*/2}\left(\int_{S_c^{(1)}} p_n^{+}\,\dot{w}_{1,n}^{+}dS\right)\mathrm{d}\tau + \frac{1}{2}\sum_{i=1}^{1}\int_{T_*/2}^{T_*}\left(\int_{S_c^{(1)}} p_n^{-}\,\dot{w}_{1,n}^{-}\,\mathrm{d}S\right)\mathrm{d}\tau \tag{12}$$

and for $\tilde{\beta}_1 \neq 0$, $\tilde{\beta}_2 = 0$, $a_1 = b_1 = 1$ there is

$$\frac{E_w}{2u_0\,\tilde{\beta}_1} = \int\limits_{S_c^{(1)}} \{\,\left(p_n^+\right)^2 + \left(p_n^-\right)^2\,)\}\,dS = \frac{E_w^+}{2u_0\,\tilde{\beta}_1} + \frac{E_w^-}{2u_0\,\tilde{\beta}_1}\,. \tag{13}$$

In the steady wear state $E_w$ reaches a minimum value. Let us note that $p_n^+$ and $p_n^-$ are not uniformly distributed at the contact interface. Taking the coordinate $\tilde{x} = 1130 - x$ it can be stated that $p(x) = p(\tilde{x})$ during the consecutive semi-cycles of reciprocal sliding.

It is very important that during the steady wear periodic state the wear increment accumulated during one cycle should be compatible at each point $p(x) = p(\tilde{x})$ with the rigid body punch motion. The main idea for derivation of the wear increment and summed pressure for $2D$ system with cylindrical contact surface is collected in the Appendix.

Assume the rigid body wear velocities for left $(-)$ and right $(+)$ directions of the substrate in the following

$$\dot{\boldsymbol{\lambda}}_F^- = -\dot{\lambda}_F^-\,\boldsymbol{e}_z\,, \quad \dot{\boldsymbol{\lambda}}_M^- = \dot{\lambda}_M^-\,\boldsymbol{e}_y\,, \quad \dot{\boldsymbol{\lambda}}_F^+ = -\dot{\lambda}_F^+\,\boldsymbol{e}_z\,, \quad \dot{\boldsymbol{\lambda}}_M^+ = -\dot{\lambda}_M^+\,\boldsymbol{e}_y\,. \tag{14}$$

Thus the velocities at an arbitrary point at the punch, Figure 2b, are $-(\dot{\lambda}_F^+ + \dot{\lambda}_M^+\tilde{x})\boldsymbol{e}_z$, or $-(\dot{\lambda}_F^- - \dot{\lambda}_M^-\tilde{x})\boldsymbol{e}_z$. The displacements resulting from this velocities are

$$-\,(\Delta\lambda_F^+ + \Delta\lambda_M^+\tilde{x})\boldsymbol{e}_z \quad \text{and} \quad -\,(\Delta\lambda_F^- - \Delta\lambda_M^-\tilde{x})\boldsymbol{e}_z \tag{15}$$

where

$$\Delta\lambda_{F,M}^+ = \int\limits_0^{T_*/2} \dot{\lambda}_{F,M}^+\,dt\,, \quad \Delta\lambda_{F,M}^- \int\limits_{T_*/2}^{T_*} \dot{\lambda}_{F,M}^-\,dt\,.$$

Thus, the total wear accumulated during one sliding cycle is

$$\Delta w_n = \Delta w_n^+ + \Delta w_n^- = (\Delta\lambda_F^- + \Delta\lambda_F^+) - (\Delta\lambda_M^- - \Delta\lambda_M^+)\,\tilde{x}\,. \tag{16}$$

This value of wear can be calculated from the wear law supposing $\tilde{\beta}_1 \neq 0$, $\tilde{\beta}_2 = 0$, $a_1 = b_1 = 1$, thus according to (A.12)

$$\Delta w_n = \Delta w_n^+ + \Delta w_n^- = Q\;(p_n^+ + p_n^-) = 2\,Q\,p_m = Q\,p_\Sigma \tag{17}$$

where

$$p_m = (p_n^+ + p_n^-)/2 = p_\Sigma/2 \quad \text{and} \quad Q = \tilde{\beta}_1 \int\limits_0^{T_*/2} \|\dot{\boldsymbol{u}}_\tau\|\;dt\,.$$

Comparing (16) and (17), it is seen that the distribution of the sum of contact pressure values of consecutive semi-cycles must be a linear function of position, thus

$$p_m = p_m^C + p_m^L\,\tilde{x}\,. \tag{18}$$

that is

$$\Delta w_n = \Delta w_n^+ + \Delta w_n^- = (\Delta\lambda_F^- + \Delta\lambda_F^+) - (\Delta\lambda_M^- - \Delta\lambda_M^+)\,\tilde{x} = \tilde{\beta}_1 \int_0^{T_*} \|\dot{\boldsymbol{u}}_\tau\|\, dt\; 2\,(p_m^C + p_m^L\,\tilde{x}),$$

where $\Delta\lambda_{F,M}^{\pm}$ is the increment of rigid body wear velocities in the half period time. Using the equilibrium equations for summed loads, the summed pressure for the steady wear state is determined as

$$p_m^C = \frac{F_0}{S_c} - \frac{3F_0(-L+2\tilde{x}_F)}{L\,S_c}\,, \quad p_m^L = \frac{6F_0(-L+2\tilde{x}_F)}{L^2\,S_c}\,, \qquad p_\Sigma = 2p_m = p_n^+ + p_n^- = 2(p_m^C + p_m^L\,\tilde{x}) \tag{19}$$

where $\tilde{x}_F$ is the coordinate of the resultant load $F_0 = F_0(p^\sim)$ . For non-negativity of $p_m$ there should be $L/2 \leqslant \tilde{x}_F \leqslant 2L/3$. At $\tilde{x}_F = L/2$ the results of [5, 6] are obtained. Here $S_c$ is the area of contact zone.

The wear increment in one period (note that the contact pressure is fixed in half period) equals

$$\Delta w_{1,n} = \tilde{\beta}_1 \left[p_n^+ + p_n^-\right](u_0\omega) \int_0^{T_*/2} |\sin\,\omega\tau|\;\mathrm{d}\tau\,, \tag{20}$$

which using (11) provides the simple relation

$$\Delta w_{1,n} = \tilde{\beta}_1 \left[p_n^+ + p_n^-\right]\; 2u_0 = Q\; p_\Sigma\,, \tag{21}$$

where $Q = \tilde{\beta}_1\; 2u_0$ and the averaged wear rate in one period equals

$$\bar{\dot{w}}_{1,n} = \frac{\Delta w_{1,n}}{T_*} = \frac{\tilde{\beta}_1[p_n^+ + p_n^-]}{T_*} 2u_0\,. \tag{22}$$

If the rigid body wear velocity $\lambda_M^+ = \lambda_M^- = 0$, (at the supports – see Figure 2a), then in the steady periodic wear regime the uniform wear increment is accumulated during full cycle at each point of the contact zone and the following condition should be satisfied:

$$p_n^+ + p_n^- = 2p_m = const\,. \tag{23a}$$

*Remark*: If $a_1 = 1$ $b = b_1 \neq 1$ then in a periodic steady state there must be

$$\left(p_n^+\right)^{\,b} + \left(p_n^-\right)^{\,b} = 2(p_m)^{\,b} = const2 \tag{23b}$$

where $p_m$ is the contact pressure at the center of the punch contact zone, at $x = 1100$. Because at $x = 1070$, $p_n^- = 0$ the contact pressure is

$$p_n^+(x = 1070) = 2^{1/b} p_m \tag{23c}$$

At the other perimeter at $x = 1130$ it holds that $p_n^+ = 0$ and

$$p_n^-(x = 1130) = 2^{1/b} p_m\,. \tag{23d}$$

Performing time integration of the wear rate rule for $a_1 = b_1 = 1$ during the one half period, the wear increment is calculated in the following way:

$$\Delta w_{1,n}^{(j)} = \int_{t_p}^{t_p+T_*/2} \tilde{\beta}_1 \, p_n^{(j)}(\tau) \; u_0 \, \omega \; |\sin \omega\tau| \; \mathrm{d}\tau \cong \tilde{\beta}_1 \, p_n^{(j)}(t_p + T_*/2) \int_0^{T_*/2} u_0 \omega \; |\sin \omega\tau| \; \mathrm{d}\tau \tag{24}$$

where $t_p$ is the time of start of the half period, $p_n^{(j)} = p_n^{(j)}(t_p + T_*/2)$.

The accumulated wear at the end of half period at the iterational step $j$ equals

$$w_{1,n}^{(j)}(t_p + T_*/2) = w_{1,n}(t_p) + \Delta w_{1,n}^{(j)} = w_{1,n}(t_p) + \tilde{\beta}_1 \, p_n^{(j)} \; 2 \; u_0 \tag{25}$$

or in other notation

$$w_{1,n}^{(j)}(t_p + T_*/2) = {}^{t_p+T_*/2}w_{1,n}^{(j)} = {}^{t_p}w_{1,n} + \Delta w_{1,n}^{(j)} \, . \tag{26}$$

This $j$ type iterational process is repeated until $j = J$ when the following convergence criterion for contact shape is satisfied, thus

$$e_w = 100 \left| \int_{S_c} \left( {}^{t_p}g + \Delta w_{1,n}^{(j)} \right) dS - \int_{S_c} \left( {}^{t_p}g + \Delta w_{1,n}^{(j-1)} \right) \, dS \right| \Big/ \int_{S_c} \left( {}^{t_p}g + \Delta w_{1,n}^{(j-1)} \right) dS \leqslant \leqslant 0.01 \, . \tag{27}$$

Here ${}^{t_p}g$ is the initial gap at the beginning of the half period.

Remark: If $a_1 = 1$, $b = b_1 \neq 1$ then the wear increment during the one half period is

$$\Delta w_{1,n}^{(j)} = \tilde{\beta}_1 \left( p_n^{(j)} \right)^b \; 2 \; u_0 \, . \tag{28}$$

In practical calculations the iterative scheme of contact pressure and wear shape correction can be modified after $k$ half cycles, so we can write

$${}^{t_p+kT_*/2}w_{1,n} = {}^{t_p}w_{1,n} + k\Delta w_{1,n}^{(J)} \, . \tag{29}$$

In our case we chose the extrapolation factor $k$ in the following way:
for the numerical steps $n \leq 50$, $k = 1$; for $50 < n \leq 100$, $k = 5$ and when $n > 100$, then $k = 10$.

The number of the half periods in the interval then is

$$\begin{aligned} &50 \leqslant n \leqslant 100 \quad && n_{hp} = 50 + (n - 50) \cdot 5 \, , \\ &n \geqslant 100 && n_{hp} = 300 + (n - 100) \cdot 10 \, . \end{aligned} \tag{30}$$

## 5. Examples

5.1. **Example 1: wear of punch induced by periodic sliding of the substrate.** Let us analyze the wear of the punch (Body 1) shown in Figure 2. We would like to examine two types of constraints, one when the punch can move only in the vertical direction (see Figure 2a), and second when the punch has additional rotation around a pin (see Figure 2b). The point $M$ in the punch has coordinates: $x = 1070$, $z = 100$.

The following geometric parameters are assumed: the punch width is $L = 60$ mm, its height is $h = 100$ mm, the thickness of punch and strip is $t_{th} = 10$ mm.

The wear parameters are: $\tilde{\beta}_1 = 1.25\pi{\cdot}10^{-8}$, $\tilde{\beta}_2 = 0$, $a_1 = 1$, $b_1 = 1$, the coefficient of friction is $\mu = 0.25$. The horizontal displacement of the substrate is $u_\tau = -u_0 \cos\omega\tau$, where $u_0 = 1.5$ mm, $\omega = 10$ rad/s, $\tau$ is the time. The material parameters are presented in Table 1.

Table 1. Mechanical parameters of two materials

| | Young modulus MPa | Poisson ratio | Material density kg/m$^3$ |
|---|---|---|---|
| Material 1 (steel) | $2.0 \times 10^5$ | 0.30 | 7800 |
| Material 2 (composite) | $1.3 \times 10^5$ | 0.23 | 846 |

The upper parts of the punch and strip are assumed to be made of the same material, (Material 1, see Table 1). The lower punch portion of height 20 mm is characterized by the parameters of Material 2 (see Table 1).

5.1.1. *Symmetric load.* The punch is loaded on the upper boundary $z = 200$ mm by the uniform pressure $p^{\sim} = 16.666$ MPa corresponding to the resultant vertical force $F_0 = 10.0$ kN.

*The wear parameter is* $b = 1$. This problem was neglecting the heat generation in [13], and accounting for heat generation in [15]. The numerical results of paper [13] are collected in Table 2 and in Figure 4 for $l_z = 40$mm.

Let us denote the contact pressure for the punch of Figure 2a by $p_n(\dot{\lambda}_F)$, for the punch of Figure 2b for $l_z = 20$ and $l_z = 40$ by $p_n(\dot{\lambda}_F, \dot{\lambda}_M, l_z = 20)$ and $p_n(\dot{\lambda}_F, \dot{\lambda}_M, l_z = 40)$, respectively.

After time integration of the Archard wear rule the contact pressures at point M are collected in Table 2 versus the numerical time steps $n$ for different punch constraints.

It is clear that convergence to the pressure 33.333 MPa proceeds for all cases of constraints. In the case $l_z = 40$mm the evolution of the shape and contact pressure is demonstrated in Figure 4.

Because the loading distribution is symmetric, the distribution of the pressure and shape is also symmetric. The optimal solutions (marked by ...) correspond to the monotonic relative motion. Also it is observed that after $n \geq 1500$ the pressure distribution does not change and the contact profile is preserved, moving along the punch axis like a rigid line. In this case $\Delta\lambda_F^- = \Delta\lambda_F^+, \Delta\lambda_M^- = \Delta\lambda_M^+$, that is in the wear process the accumulated punch wear is the same during each period, the pressure distribution is $p_m = p_m^C = p^{\sim}$, and the summed pressure $p_\Sigma = p_n^+ + p_n^- = 2p_m = 2p^{\sim}$.

Table 2. Contact pressure at the point $M$ versus numerical time steps $n$

| $n$ | no. of half period $n_{hp}$ | $p_n(\dot{\lambda}_F)$ | $p_n(\dot{\lambda}_F, \dot{\lambda}_M, \ell_z = 20)$ | $p_n(\dot{\lambda}_F, \dot{\lambda}_M, \ell_z = 40)$ |
|---|---|---|---|---|
| 1 | 1 | $0.14841933E+03$ | $0.10087461E+03$ | $0.13837226E+03$ |
| 50 | 50 | $0.11470731E+03$ | $0.87926576E+02$ | $0.10745308E+03$ |
| 100 | 300 | $0.69721237E+02$ | $0.57950338E+02$ | $0.67301651E+02$ |
| 200 | 1300 | $0.46654939E+02$ | $0.41195687E+02$ | $0.46039272E+02$ |
| 300 | 2300 | $0.40931186E+02$ | $0.36462991E+02$ | $0.40376545E+02$ |
| 400 | 3300 | $0.37501127E+02$ | $0.35565594E+02$ | $0.37620120E+02$ |
| 500 | 4300 | $0.36392637E+02$ | $0.34548895E+02$ | $0.36225178E+02$ |
| 600 | 5300 | $0.35307986E+02$ | $0.33997961E+02$ | $0.35262677E+02$ |
| 700 | 6300 | $0.34768942E+02$ | $0.33713578E+02$ | $0.34696425E+02$ |
| 800 | 7300 | $0.34330459E+02$ | $0.33562469E+02$ | $0.34205548E+02$ |
| 900 | 8300 | $0.34008547E+02$ | $0.33456073E+02$ | $0.33905548E+02$ |
| 1000 | 9300 | $0.33529593E+02$ | $0.33394566E+02$ | $0.33758886E+02$ |
| 1100 | 10300 | $0.33568957E+02$ | $0.33358149E+02$ | $0.33445945E+02$ |
| 1500 | 15300 | $0.33403968E+02$ | $0.33307992E+02$ | $0.33345945E+02$ |
| 1700 | 16300 | $0.33372654E+02$ | $0.33304515E+02$ | $0.33335945E+02$ |

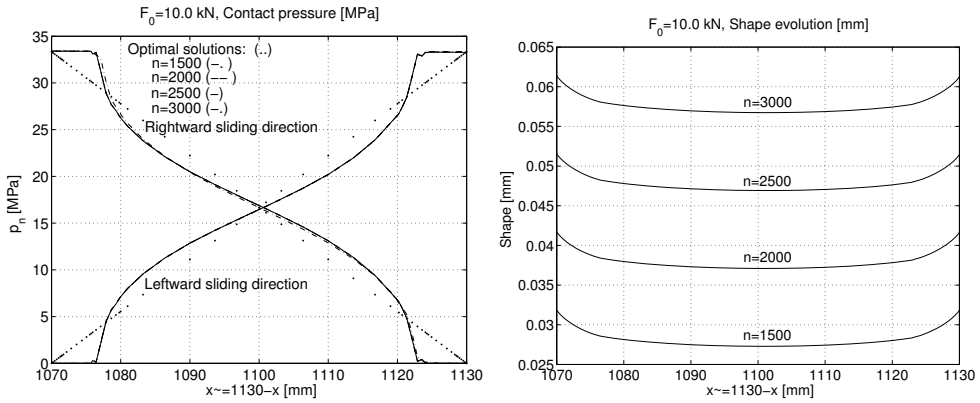


a) b)

Figure 4. a) Contact pressure at different time steps and sliding directions, b) evolution of shape of punch for reciprocal motion, $l_z = 40$ mm, the load $p^{\sim} = 16.666$ MPa and resultant force's coordinate is $\tilde{x}_F = L/2$.

*The wear parameter is* $b \neq 1$. Let us investigate the periodic wear process at $\tilde{\beta}_1 = 1.25\,\pi\,\mu^{0.2}10^{-8}$, $\tilde{\beta}_2 = 0$, and $a_1 = 1$, $b = b_1 = 1.2$, $\mu = 0.25$. The displacement of body 2 is: $u = -u_0 \cos\omega\tau$, where $u_0 = 1.5$ mm, $\omega = 10$ rad/s.

Performing time integration of (1) we see that after the number of half periods ($n \geq 1100$) $n_{hp} \geq 10300$ the wear process reaches its steady state. In this case the value $2\,(p_m)^{\,b} = const2 = 61.48$, where $p_m = 17.369$ MPa, $p_n^+ = p_n^- = 30.948$ MPa.

Comparing the contact pressure and shape of punch in the steady state, we see that the pressure for $b = 1.2$ at the border of contact zone is lower than that for $b = 1$, and at the center of the punch the pressure is higher. The contact shape for $b = 1.2$ is shown by the curve placed above that predicted for $b = 1$ (cf. Figure 5). On the other hand, for the case $b = 0.8$, the contact pressure is higher than that for $b = 1$ at the perimeter points, and the contact shape curve is lower than that for $b = 1$. It also is noted that for the wear parameter value $\tilde{\beta}_1 = 1.25\,\pi\,\mu^{-0.2}10^{-8}$, which is the smallest, the steady state is reached at $n = 2500$. Then the pressure in the center is $p_m = 15.886$ MPa, the value $2\,(p_m)^{\,b} = const2 = 18.274$, the pressure at the perimeter points are $p_n^+ = p_n^- = 37.806$ MPa and calculated value is $(p_n^+)^b = (p_n^-)^{\,b} = 18.283$. The calculation error $100\left[(p_n^+)^b - 2\,(p_m)^{\,b}\right]/2\,(p_m)^{\,b} = 0.0055$ is very small. Also $p_n^+(x = 1070) = 2^{1/b}p_m$, $p_m = 15.8954$ MPa.

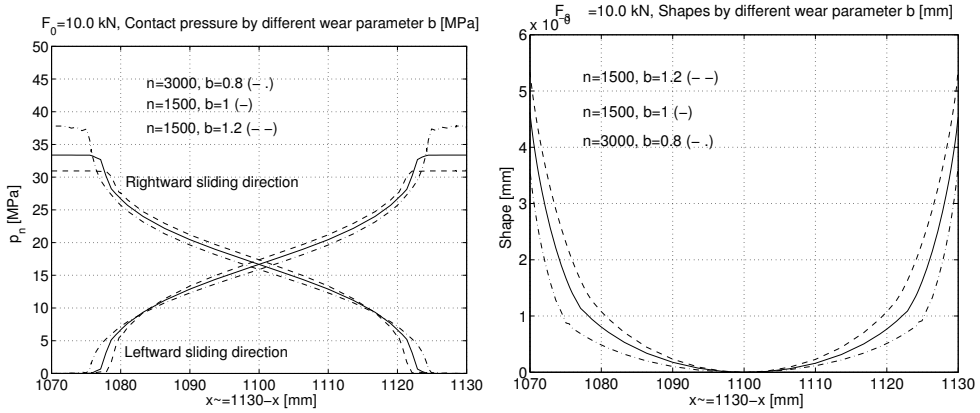


a) b)

Figure 5. The effect of the wear parameter b on the periodic steady wear state, a) distribution of the contact pressure, b) contact shape of punch (maximal shape function ordinate is 6 $\mu$m).

5.1.2. *Non-symmetric load.* Let us now analyze the case of eccentric load when the resultant vertical force equals $F_0 = 10$ kN and its position coordinate is in the interval $L/2 = 30 \le \tilde{x}_F \le 2L/3 = 40$.

*The first case.* The pressure $p^{\sim} = 20$ MPa is applied in the interval $10 \le \tilde{x} \le 60$. The resultant position coordinate is $\tilde{x}_F \le 35$ mm. This load case represents the variant 2. The results are presented in Figure 6. Figures 6a,c demonstrate the pressure at different numbers of half cycles and Figures 6b,d present the summed pressure $p_\Sigma = p_n^+ + p_n^- = 2p_m$. It is seen that after $n \ge 1000$ the summed pressure practically does not change. Its distribution is presented by a linear function. A small oscillation is observed because in the solution of the contact problem the positional technique has not been used [17]. In our calculation it is required that the gap in point $x = 1130$ mm of the contact zone be fixed during consecutive iterations. The contact shapes are shown in Figures 7a,b. If the pin height is $l_z = 20$mm, the obtained pressure

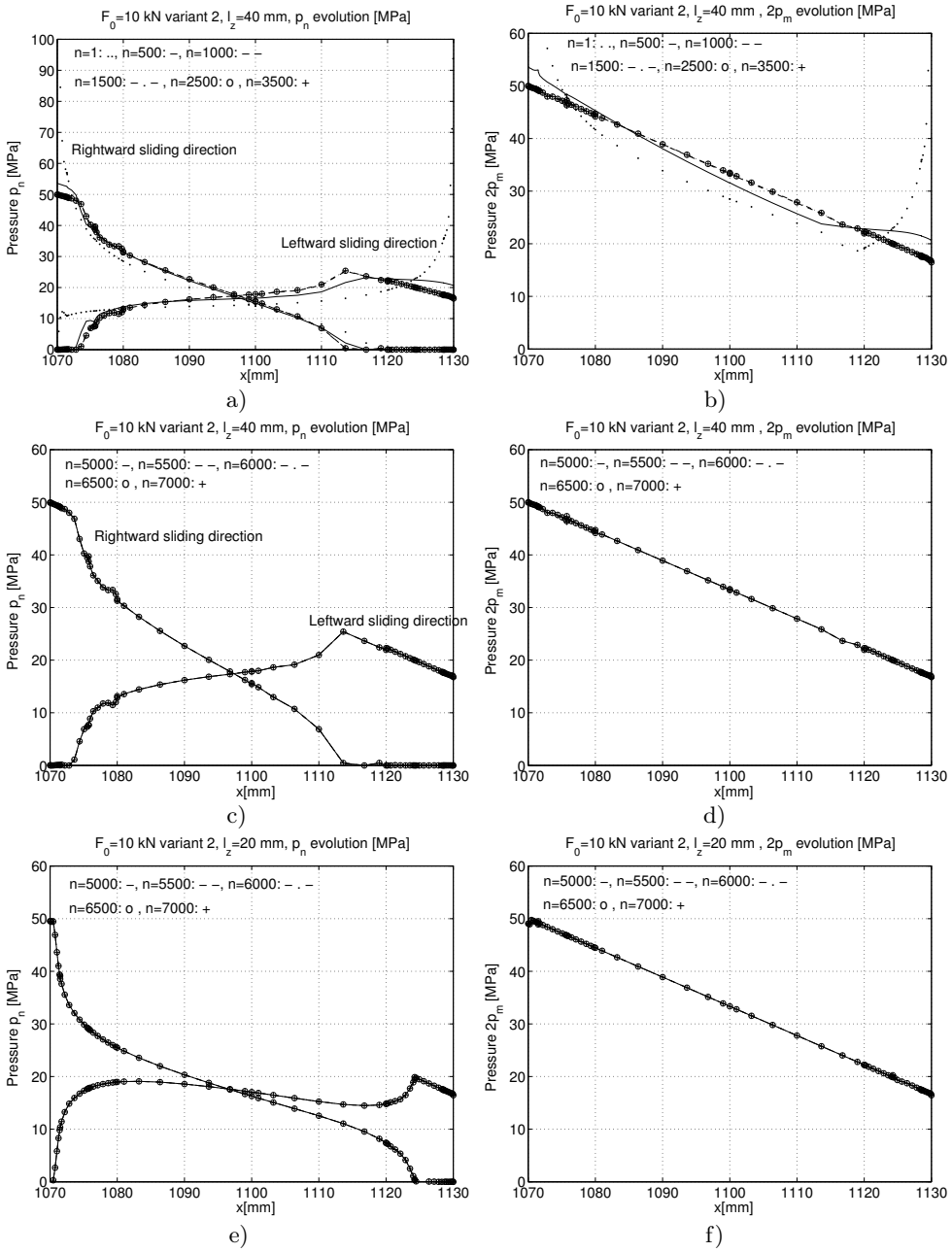


Figure 6. Periodic wear process for the load variant 2: a), c), e) evolution of pressures, b), d), f) evolution of the summed pressure $p_\Sigma = 2p_m$.

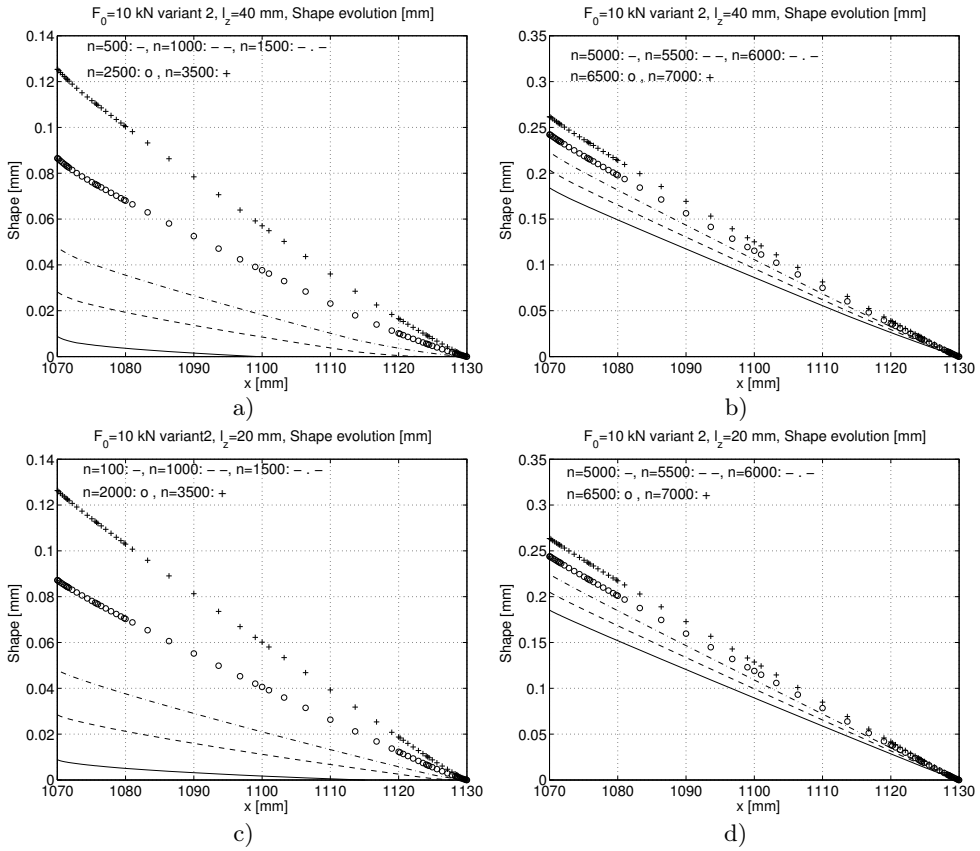


Figure 7. Evolution of contact shapes for periodic wear process at the load variant 2: a), c), $n = 100 - 3500$, b), d) $n = 5000 - 7000$.

distribution is shown in Figure 6e, and the summed pressure is shown in Figure 6f. The contact shapes are presented in Figures 7c,d. Because in the equation for summed pressure (19) the height $l_z$ is absent, the summed pressures for $l_z = 20$ mm, and $l_z = 40$ mm must be the same. This fact is also demonstrated by the numerical time integration results (compare Figures 6d and 6f).

*The second case.* The pressures $p_1^{\sim} = 25$ MPa, $p_2^{\sim} = 12.5$ MPa act in the intervals: $p_1^{\sim}$: $30 \le \tilde{x} \le 60$, $p_2^{\sim}$: $10 \le \tilde{x} \le 30$. The resultant vertical force is $F_0 = 10$ kN, the resultant position coordinate is $\tilde{x}_F \le 37.5$ mm. This load case corresponds to variant 3.

The pressure distribution can be seen in Figures 8a,c and the summed pressure in Figures 8b,d. The maximum of the pressure is higher than before, because the resultant coordinate $\tilde{x}_F$ is larger by 2.5 mm. In this case the high pressure at the border of contact domain very quickly decreases. For the periodic steady wear state the maximum of the pressure can be calculated from the summed pressure, which is predicted without time integration! For each half period the contact gap has been

specified. For the rightward sliding direction the maximum of the contact pressure is on the left border of contact zone, but for the leftward sliding direction the maximum is in the interior of the contact zone.

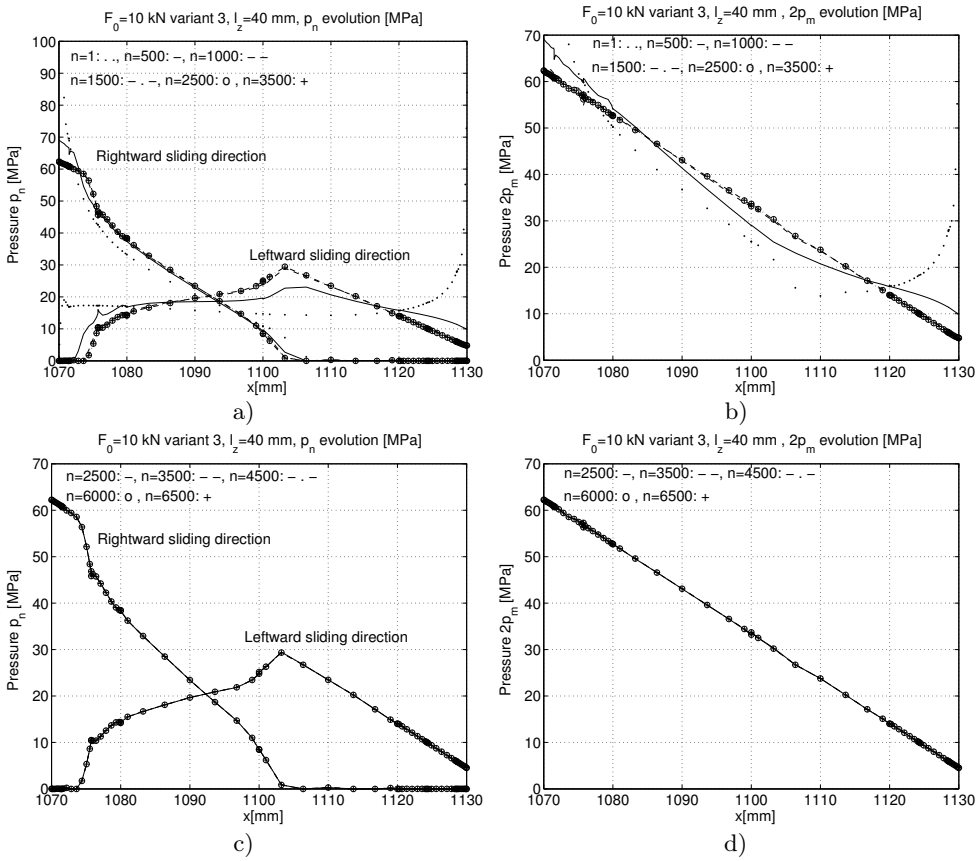


Figure 8. Periodic wear process for the load variant 3: a), c) evolution of the pressures, b), d) evolution of the summed pressure $p_\Sigma = 2p_m$.

The wear is larger for loading variant 3 than for the variant 2. However, the character of wear process is the same. The shape evolution is presented in Figures 9a,b.

5.2. **Example 2: Periodic steady wear state for a disk brake system.** Consider the periodic tangential relative displacement of body $B_2$ (the disk) with respect to body $B_1$ in the direction $\boldsymbol{e}_\tau$

$$\boldsymbol{u}_\tau = u_0 \ \cos\omega\tau \ \boldsymbol{e}_\tau \tag{31}$$

where $u_0$ and $\omega$ are the amplitude and angular velocity of the motion.

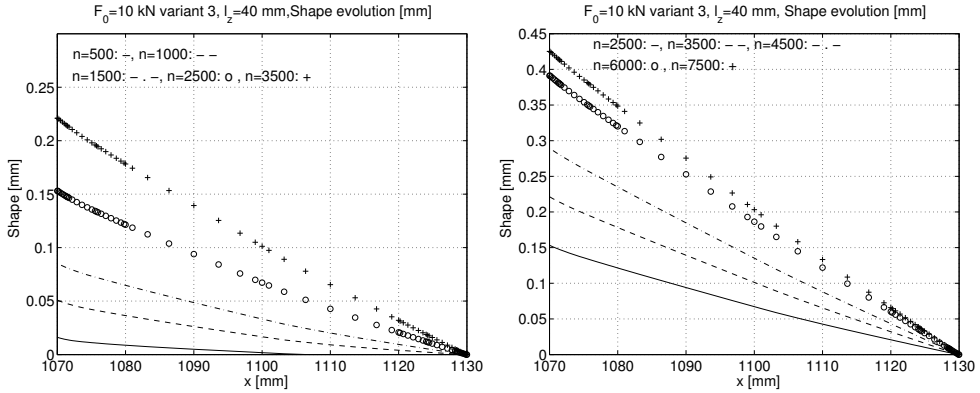


a) b)

Figure 9. Evolution of the contact shapes for periodic wear process at the load variant 3: a) $n = 500 - 3500$, b) $n = 2500 - 7500$.

The relative sliding velocity and the cycle period are

$$\dot{\boldsymbol{u}}_\tau = -u_0\,\omega \sin\omega\tau\;\boldsymbol{e}_\tau = -v_r\;\boldsymbol{e}_\tau \tag{32a}$$

$$v_r = \|\dot{\boldsymbol{u}}_\tau\| = |\omega\; u_0\;\sin\omega\tau| = |v_0\,\sin\omega\tau|\;, \quad T_* = \frac{2\pi}{\omega}\,, \quad v_0 = \omega\, u_0 \tag{32b}$$

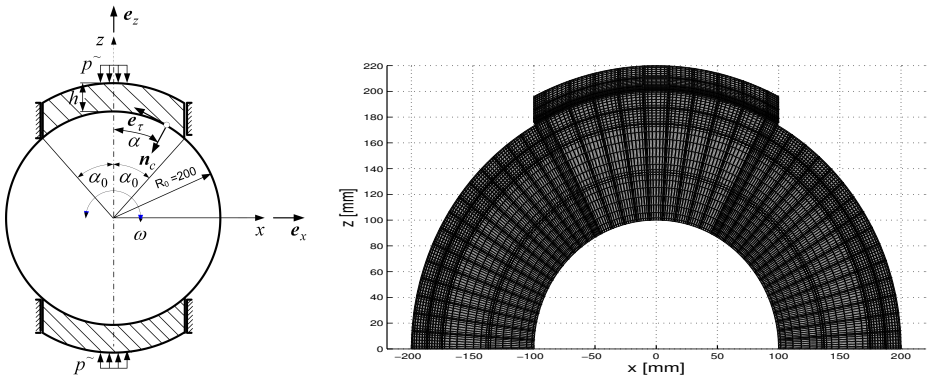


a) b)

Figure 10. Brake system, a) $\alpha_0 = 30°$, the resultant force $F_0 = 10$ kN, thickness of bodies $t_{th} = 10$ mm; b) finite element mesh of the half part of the system, number of contact elements is 11, number of elements in radial direction is 4, the $p$-version of the finite elements has $p = 8$ polynomial degree. The liners are drawn through the Lobatto integral coordinates.

The shoe (body $B_1$) is loaded by the force $\boldsymbol{F}_0 = -F_0\;\boldsymbol{e}_z$. In our case $F_0 = 10$ kN. The Lagrangian multiplier $\dot{\lambda}_F$ represents the vertical wear velocity.

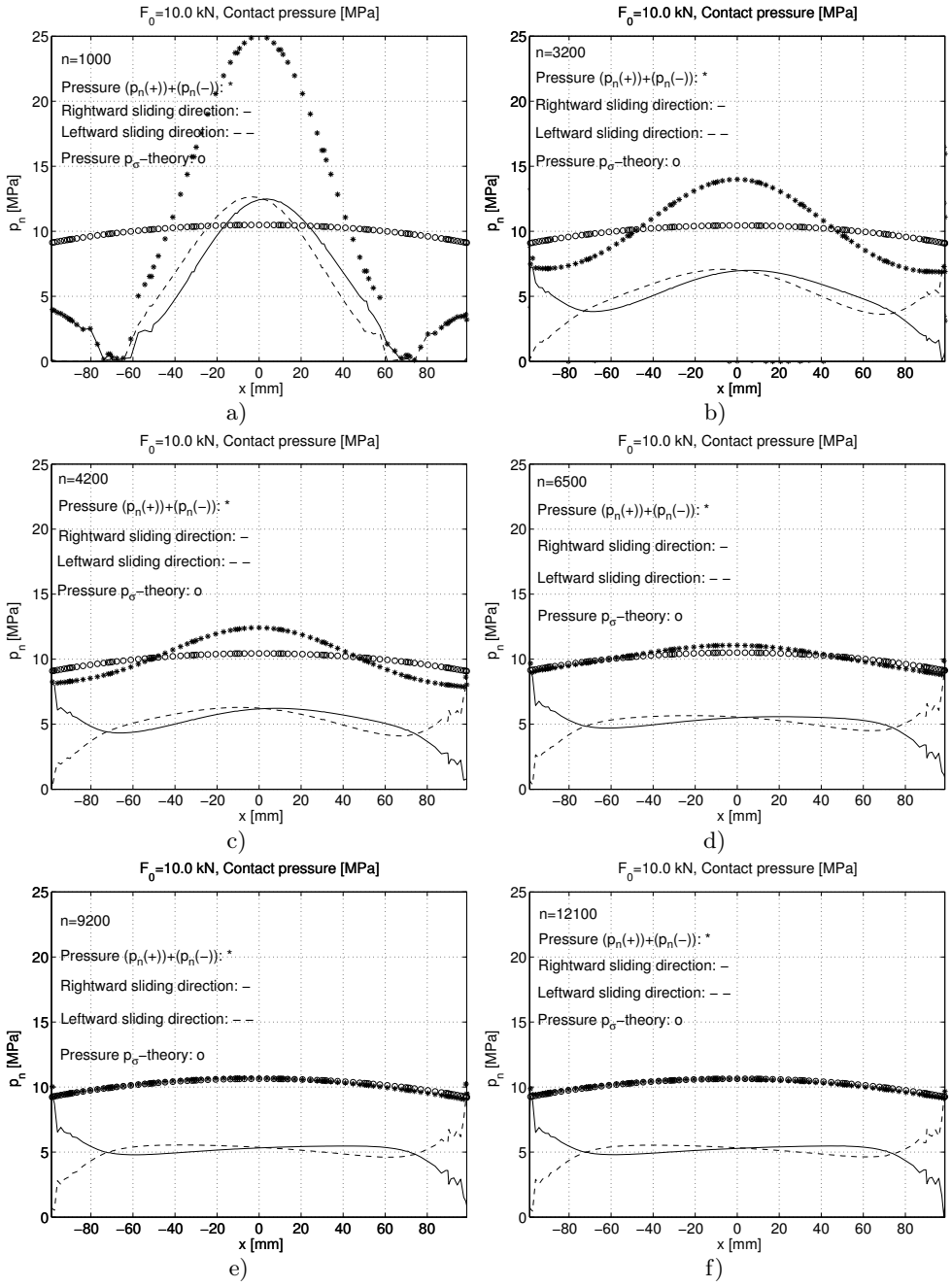


Figure 11. Contact pressure and summed pressure ($p_\Sigma = p_\sigma$ – *theory*) distribution at different time steps.

It is easy to calculate the average normal wear rate for body 1. (The normal wear vector is $\dot{\boldsymbol{w}}_{1,n} = -\dot{w}_{1,n}\boldsymbol{n}_c$)

$$\bar{\dot{w}}_{1,n} = \frac{1}{T_*}\int_0^{T_*} \tilde{\beta}_1 p_n^b v_r^{a_1}\,\mathrm{d}\tau = \frac{\tilde{\beta}_1 p_n^b}{T_*}\int_0^{T_*} v_r^{a_1}\,\mathrm{d}\tau = \tilde{\beta}_1 p_n^b \bar{v}_r^{a_1} \tag{33}$$

The vertical average wear rate is

$$\bar{\dot{w}}_R = \bar{\dot{w}}_{1,n}/\cos\alpha \tag{34}$$

In view of (32)-(34), the average vertical wear rate in one period equals

$$\bar{\dot{w}}_R = \frac{1}{\cos\alpha}\frac{\tilde{\beta}_1[p_n^{+b} + p_n^{-b}]}{T_*}(u_0\omega)^{a_1}\int_0^{T_*/2} |\sin\,\omega\tau|^{a_1}\,\mathrm{d}\tau \tag{35a}$$

which for $a_1 = b = 1$ provides the relation

$$\bar{\dot{w}}_R = \frac{1}{\cos\alpha}\frac{\tilde{\beta}_1[p_n^{+} + p_n^{-}]}{T_*}2u_0\,, \quad \Delta w_R = \bar{\dot{w}}_R T_* = \frac{1}{\cos\alpha}(p_n^{+} + p_n^{-})\tilde{\beta}_1 2u_0 \tag{35b}$$

where $\Delta w_R$ is the vertical wear increment for one motion cycle.

Let us note that $p_n^+$ and $p_n^-$ are not uniformly distributed on the contact interface. To assure the uniform wear increment $\Delta w_R$ accumulated during full cycle at each point of the contact zone, the following condition should be satisfied according to results of (A.20) in the Appendix:

$$\Delta w_R = \frac{\Delta w_{1,n}}{\cos\alpha} = \frac{Qp_\Sigma}{\cos\alpha} = Q2p_m^C = const \tag{36}$$

where

$$p_\Sigma = p_n^+ + p_n^- = 2p_m = 2p_m^C\cos\alpha\,, \quad Q = \tilde{\beta}_1\,2u_0 \tag{37}$$

The wear parameters are $\tilde{\beta}_1 = 0.5\pi\cdot 10^{-8}$, $\tilde{\beta}_2 = 0$, $a_1 = b_1 = 1$. The sliding parameters are $u_0 = 1.5$ mm, $\omega = 10$ rad/s. Using time integration of the wear rule in the usual way, the obtained contact pressure evolution is demonstrated in Figure 11 at the beginning of numerical steps $n = 1000$. The number of the half periods is calculated by (10).

With increasing number of cycles condition (37) is progressively better satisfied, see Figure 11. Here $p_\Sigma = p_\Sigma(\alpha) = (p_n^+ + p_n^-) = 2p_m^C\cos\alpha$. At $n = 4200$, $p_\Sigma(0) = 12.42$ MPa, at $n = 6500$ $p_\Sigma(0) = 11.67$ MPa , at $n = 7200$ $p_\Sigma(0) = 10.93$ MPa , at $n = 8700$ $p_\Sigma(0) = 10.71$ MPa, at $n = 9200$ $p_\Sigma(0) = 10.69$ MPa, at $n = 10000$ $p_\Sigma(0) = 10.66$ MPa and at $n = 12100$ $p_\Sigma = 10.62$ MPa, that is $n \Rightarrow \infty$ $p_\Sigma(0) = 2p_m^C$. The value of $p_\Sigma(0)$ as the function of $n$ is demonstrated in Figure 12. At the beginning of the wear process the drop in pressure $p_\Sigma(0)$ is very high, next it exponentially decreases to the value $p_\Sigma(0) = 2p_m = 10.57$ MPa. This value is calculated from (A.15).

The evolution of the contact shape is also interesting. In the initial phase the wear is high in the middle contact portion, and next the shape tends to its steady form, which translates vertically as a rigid line, see Figure 13.

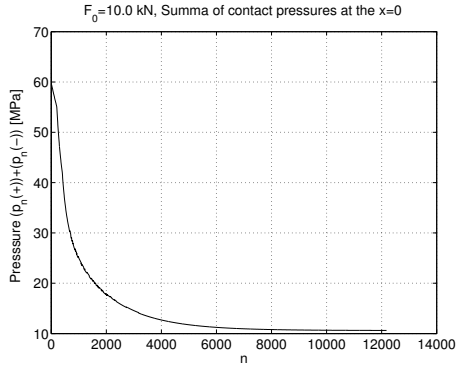


Figure 12. Satisfying the constraint of uniform vertical wear increment.

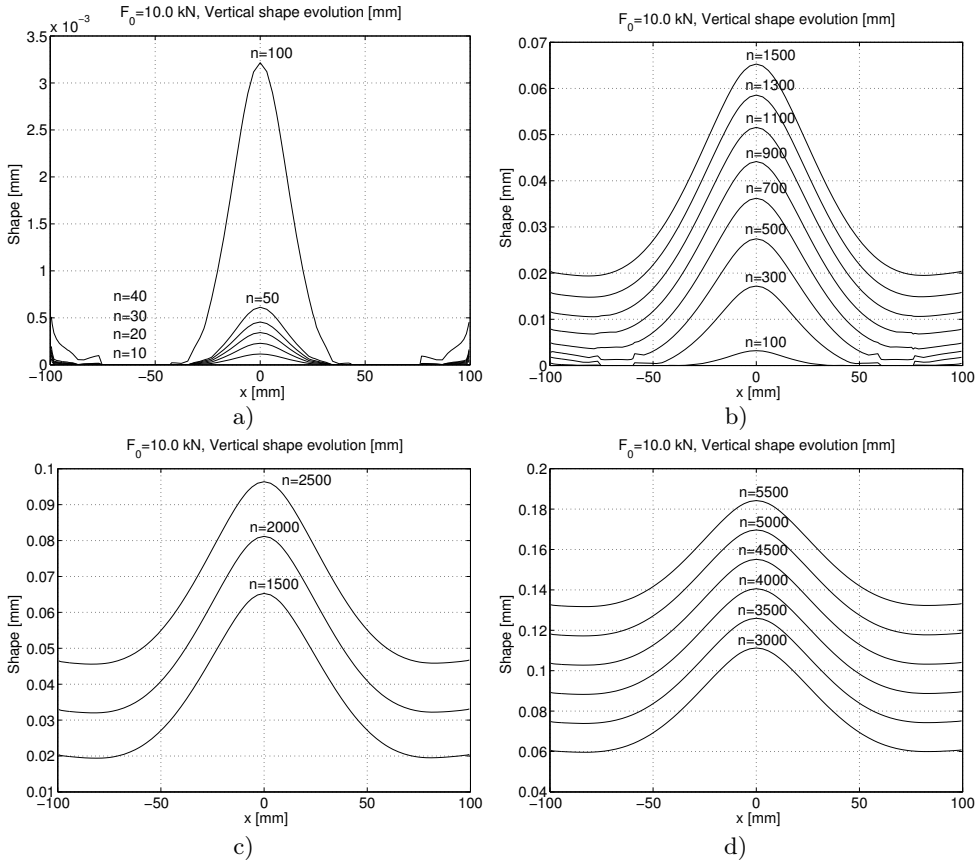


Figure 13. Evolution of contact shape in the wear process.

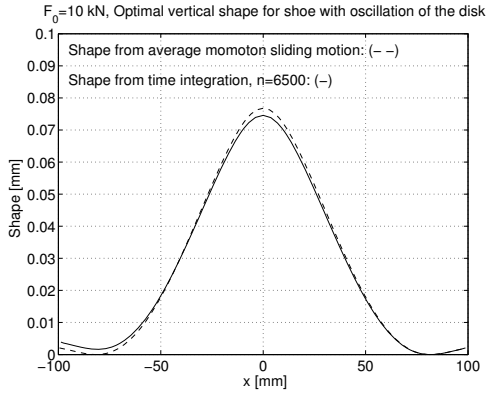


Figure 14. Prediction of contact shape from the averaged monotonic sliding motion between the shoe and disk.

The averaging technique for prediction of the shape form [13] provides an overestimated wear form, see Figure 14. In [13] it was demonstrated that the shape does not depend on the coefficient of friction. At the center point the averaged shape function has the value 0.07503 mm, and the shape function obtained by time integration of the wear rule has the value 0.07456 mm. The error is less than 1%. A small asymmetry has been found from time integration.

## 6. Optimization problem

6.1. **Specification of the initial wear form.** Let us analyze the wear of the punch (Body 1) shown in Figure 2a. We would like to find the steady contact shape for periodic motion using the results of monotonic strip sliding in the leftward or rightward direction and develop a new optimization technique. The punch now is allowed to execute a rigid body wear velocity $\dot{\lambda}_F$ [13, 15] which is normal to the contact interface. The optimal pressure for steady wear state is uniform, $p_n^+ = p_n^- = p^{\sim}$. The calculation of the initial gap that is the wear shape is performed by loading separately each body by the optimal contact pressure and friction stress. In this case the bodies are not allowed rigid body motion in the vertical direction. For monotonic sliding the equation requiring the total contact gap to vanish specifies the wear gap $g$, thus

$$d = u_n^{(2)} - u_n^{(1)} - \lambda_F + g = 0 \tag{38}$$

where the rigid body wear velocity of the punch is known from the stationary condition, so that $\lambda_F = \dot{\lambda}_F t_s$, where $t_s$ is the selected time instant specifying initiation of the steady state. The steady state shapes can be found in Figure 15, where at leftward sliding it is set at $g(x = 1070) = 0$, and at rightward sliding set at $g(x = 1130) = 0$.

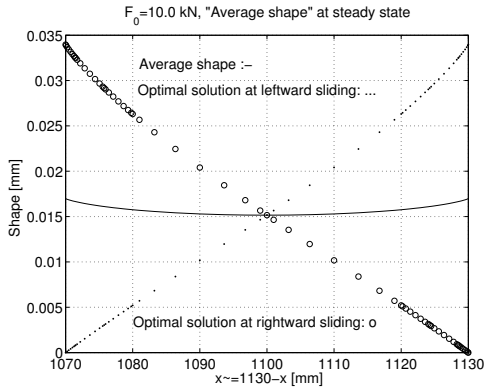


Figure 15. Shapes for the steady wear states induced by the strip monotonically translating in leftward or rightward directions. The average shape is $Shape^{(a)}$

Denoting by $shape^{(l)}$, $shape^{(r)}$ the resulting wear shape curves during the leftward and rightward monotonic sliding (see Figure 15), assume the shape curve for reciprocal

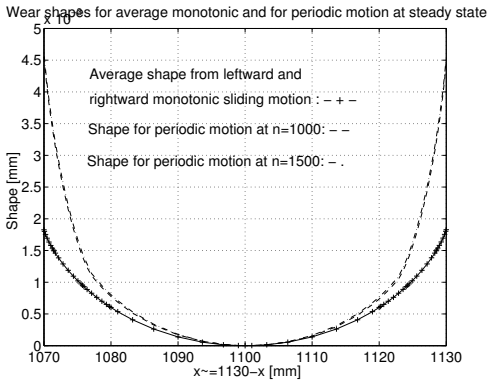


Figure 16. Prediction of the wear shape for periodic wear process from the results of monotonic sliding. The average shape is $Shape^{(a)}$

sliding to be approximated by the sum of monotonic shape curves, thus

$$Shape^{(a)} = shape^{(l)} + shape^{(r)} - 2 \cdot shape^{(l)}(x = 1100) \,, \tag{39}$$

where the last term specifies the translation of the curve along the $z$-axis in order to obtain the zero value at the mid contact point (see Figure 16). It is seen that the prediction is not close to the actual wear form at the contact edges. It is also noted that shapes at $n = 1000$ and $n = 1500$ are practically the same, so the wear process has reached its steady state at $n = 1000$.

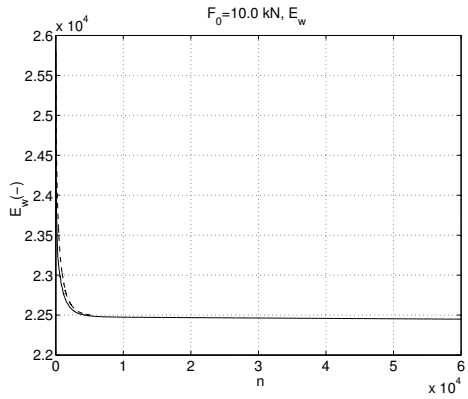


Figure 17. Evolution of the wear dissipation $E_w^-/2u_0\tilde{\beta}_1 = \int\limits_{S_c} (p_n^-)^2 dS$

The evolution of the wear dissipation energy for one cycle is plotted in Figure 17. The continuous line corresponds to the leftward and the dotted line to the rightward sliding direction of the substrate. The wear dissipation energy very quickly decreases and tends to its minimum level.

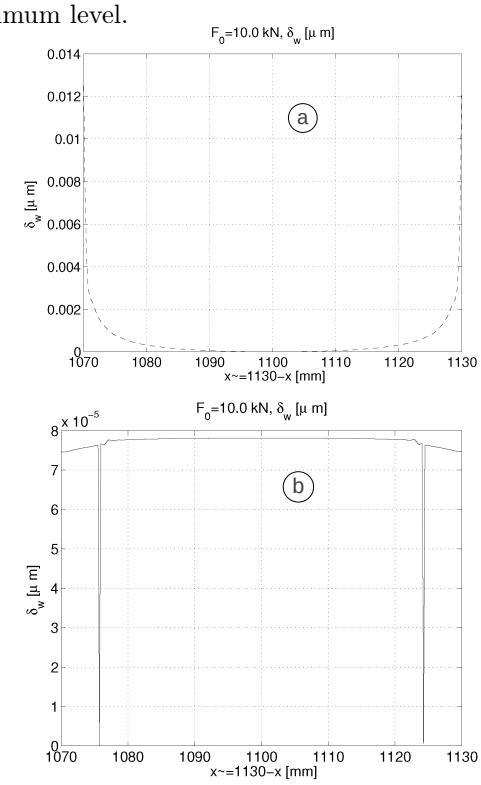


Figure 18. $\delta w = \Delta w_{1,n} - \min \Delta w_{1,n} = (\Delta w_{1,n}^+ + \Delta w_{1,n}^-) - \min(\Delta w_{1,n}^+ + \Delta w_{1,n}^-)$ at different time periods, a) at the beginning of the wear process, b) in the steady state.

Theoretically calculating the value

$$\delta w = \Delta w_{1,n} - \min \Delta w_{1,n} \tag{40}$$

it is expected that in the steady state it must vanish. Here $\delta w$ is the wear difference after one sliding period. In Figure 18 the evolution of $\delta w$ is shown at the beginning of the wear process (a), and at the periodical steady state (b). In the initial period of the wear process, $\delta w$ is ∼100 times greater than that at the steady state. In the steady state it reaches a stabilized small value. It seems to be impossible to reduce $\delta w$ to zero in the numerical calculation process.

6.2. **Solution of the optimization problem using splines.** In view of the preceding analysis, the following optimization problem can be stated for calculation of the wear shape

$$\min_{g_n} \{ \max \delta w = \Delta w_{1,n\ \max} - \Delta w_{1,n\ \min} \mid p_n^{\pm} \geq 0,\ \ d_n^{\pm} \geq 0, \\ p_n^{\pm} d_n^{\pm} = 0,\ \ \tau_n^{+} = \mu p_n^{+},\ \ \tau_n^{-} = -\mu p_n^{-},\ \ \boldsymbol{f} = \boldsymbol{0},\ \ \boldsymbol{m} = \boldsymbol{0} \} \tag{41}$$

where $\Delta w_{1,n\ \max}, \Delta w_{1,n\ \min}$ are the maximum and minimum values of wear attained in one cycle, $\boldsymbol{f} = \boldsymbol{0}$, $\boldsymbol{m} = \boldsymbol{0}$ are the punch equilibrium equations.

The global equilibrium conditions for the body $B_1$ can be expressed as (8).

According to Signorini contact conditions in the normal direction the contact pressure must be positive in the contact zone and distance after deformation between the bodies must also be positive, thus

$$d_n^{\pm} = u_n^{(2)\pm} - u_n^{(1)\pm} + g_n \geq 0 \tag{42}$$

where $u_n^{(i)} = \boldsymbol{u}^{(i)} \cdot \boldsymbol{n}_c$ is the normal displacement of the $i$-th body, $g_n$ is the initial gap (shape of body 1 in the periodic steady state which is not given, but must be found in the optimization process). The Signorini conditions for the whole period then are

$$p_n^{\pm}\, d_n^{\pm} = 0,\ \ p_n^{\pm} \geq 0,\ \ d_n^{\pm} \geq 0\,. \tag{43}$$

The objective function can be stated as $I_{\delta w} = \int_{S_c} \delta w\, dS$, or $I_{\delta w} \cdot \max \delta w$. The steady state condition then is $I_{\delta w} = 0$, also $\max \delta w = 0$. Numerically this extremum cannot be reached. In our examples it is found that $I_{\delta w} \cdot \max \delta w \sim 10^{-6}$.

6.2.1. *First step in the solution of the optimization problem* (41). The optimization problem is solved in two steps.

A. First we take the average shape for monotonic motions [5], see Figure 16(-+) line, to build a cubic spline for the following points:

| | $x$ mm | Shape mm |
|---|---|---|
| 1 | 0.10700000E+04 | 0.18265000E-02 |
| 2 | 0.10707500E+04 | 0.16335910E-02 |
| 3 | 0.10715000E+04 | 0.14934270E-02 |
| 4 | 0.10736300E+04 | 0.11869800E-02 |
| 5 | 0.10757500E+04 | 0.95190000E-03 |
| 6 | 0.10778800E+04 | 0.76108000E-03 |
| 7 | 0.10800000E+04 | 0.60226500E-03 |
| 8 | 0.10900000E+04 | 0.13810000E-03 |
| 9 | 0.11000000E+04 | 0.00000000E-00 |
| 10 | 0.11136300E+04 | 0.26240500E-03 |
| 11 | 0.11200000E+04 | 0.60244000E-03 |
| 12 | 0.11221300E+04 | 0.76135000E-03 |
| 13 | 0.11242500E+04 | 0.95234000E-03 |
| 14 | 0.11263800E+04 | 0.11876850E-02 |
| 15 | 0.11285000E+04 | 0.14945845E-02 |
| 16 | 0.11292500E+04 | 0.16349025E-02 |
| 17 | 0.11300000E+04 | 0.18279500E-02 |

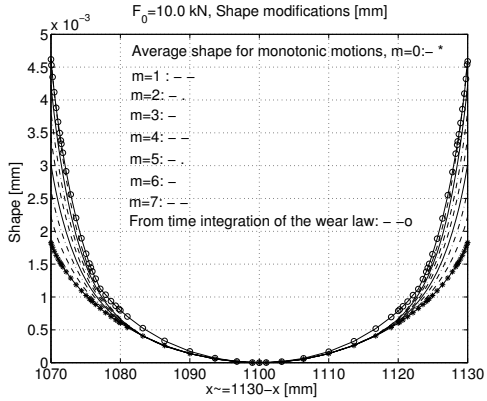


Figure 19. Shape modification specified with 9th polynomial order.

B. Then transform the data in the following way:

$$\begin{aligned} &\Delta \cdot m \cdot (x-1100)^q / (L/2)^q \quad \text{for } x \le 1100\,, \\ &\Delta \cdot m \cdot (-x+1100)^q / (L/2)^q \quad \text{for } x < 1100\,. \end{aligned} \tag{44}$$

We take $q = 9$, $\Delta = 0.0004$ mm, $m = 1, 2, ..., 7$. This procedure is named polynomial iteration. The shapes are demonstrated in Figure 19. In this figure the curve obtained from time integration of the wear rule (- - o) is presented. It is seen that the approximation curve at $m = 7$ is lower than the curve (- - o). That is, the spline approximation must be modified.

6.2.2. *Second step in the solution of the optimization problem* (41). In the second step we suppose that the new wear function can be approximated by the Taylor series

$$\delta w = \delta w^{(0)} + \sum_{j=1}^{16} \frac{\partial\,(\delta w)}{\partial a_j} \Delta\, a_j\,, \tag{45}$$

that is we can calculate the spline parameters $a_j$.

The derivative $\partial(\delta w)/\partial a_j$ is determined in the numerical way, so that

$$\frac{\partial(\delta w)}{\partial a_j} \approx \frac{\delta w(a_1^{(0)}, ..., a_j^{(0)} + \Delta_s, ..., a_{16}^{(0)}) - \delta w^{(0)}}{\Delta_s} . \tag{46}$$

In our case $\Delta s = 0.00002$.

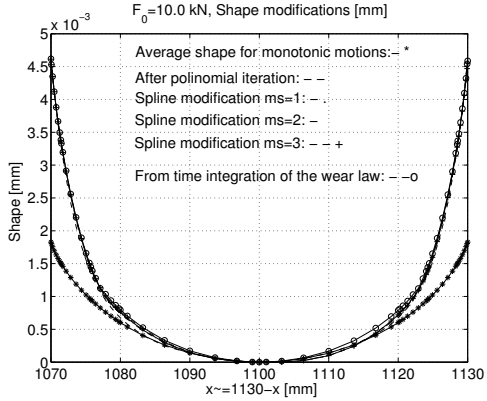


Figure 20. Shape modification specified by spline modification.

For each $j$ the contact problem must be solved and the wear is calculated for one sliding period. For the control of the condition $\delta w = 0$, 16 point zones in the contact domain are taken, and using the Raphson iteration technique, new spline point coordinates can easily be found:

$$a_j^{new} = a_j^{(0)} + \Delta a_j \tag{47}$$

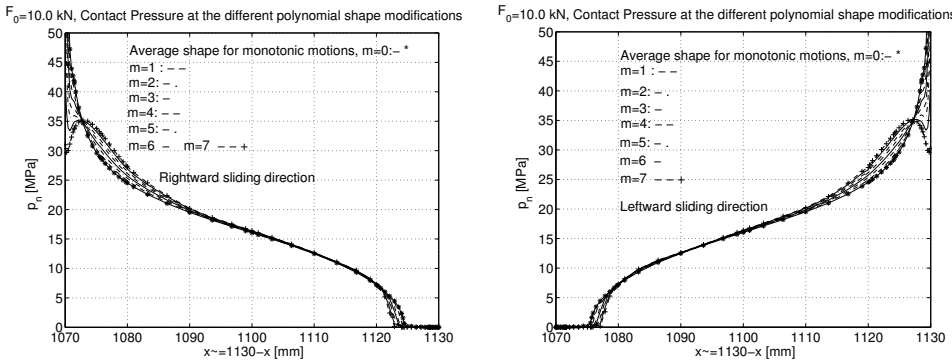


Figure 21. Contact pressure evolution due to different polynomial shape modifications, a) for rightward sliding motion, b) for leftward sliding motion.

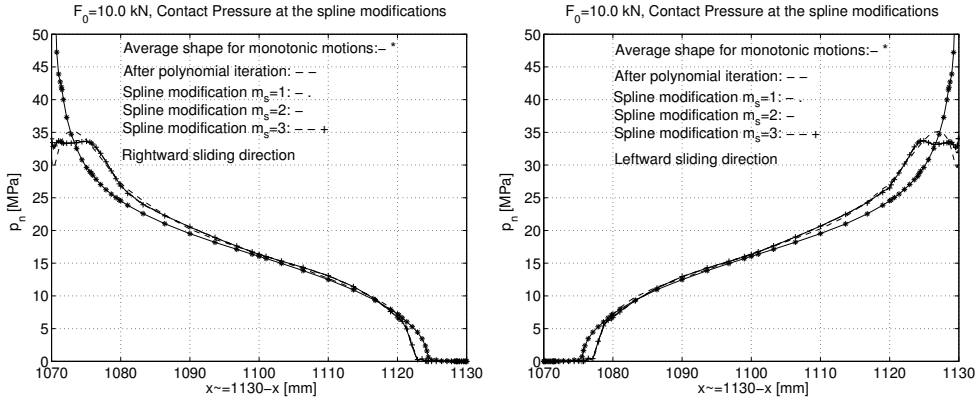


a) b)

Figure 22. Contact pressure evolution due to spline modifications, a) for rightward sliding motion, b) for leftward sliding motion.

where the algebraic system is

$$\left[\frac{\partial(\delta w)_i}{\partial a_j}\right]_{i,j=1,16}\begin{bmatrix}\Delta a_1\\ \vdots\\ \Delta a_j\\ \vdots\\ \Delta a_{16}\end{bmatrix} = -\begin{bmatrix}\delta w_1\\ \vdots\\ \delta w_j\\ \vdots\\ \delta w_{16}\end{bmatrix}^{(0)} \tag{48}$$

Using this technique, after $m_s = 1, 2, 3$ spline modifications we obtain a nice result, see Figure 20. The calculated shape is practically the same as that obtained from time integration. The contact pressure distributions are presented in Figures 21 and 22. When the averaged monotonic shape is applied, the contact pressure has a high value at the perimeter points changing with the sliding direction, see Figure 21. After polynomial iteration the pressure value is lower than that in the steady state, see lines (–+) in Figure 21. After the end of the second step, the pressure exhibits a very small oscillation, so the optimal solution is very close to the numerically specified result (see Figure 22). It can be concluded that the recommended optimization process provides correct results.

6.3. **Solution of the optimization problem by applying the penalty technique.** The objective function can be presented in a different form, using the pressure constraint in the periodic steady wear state. Define the pressure difference for the rigid body wear velocity $\dot{\lambda}_F^{\pm} \neq 0$, $\dot{\lambda}_M^{\pm} = 0$ (see (23a))

$$\Delta p_n = p_n^+ + p_n^- - 2p_m\,. \tag{49}$$

If $\Delta p_n = 0$ at each point of contact zone, then the corresponding contact shape is correct. If not, then the shape must be modified. Using the idea of penalty technique [18], we can write

$$\Delta p_n = p_n^+ + p_n^- - 2p_m = c_n(u_n^+ + g_n^+ + u_n^- + g_n^-) - 2p_m\,, \tag{50}$$

where $g_n^+$ and $g_n^-$ are the shapes (gaps) at the end of the + or – sliding direction , $c_n$ is the penalty parameter used for the normal contact problem.

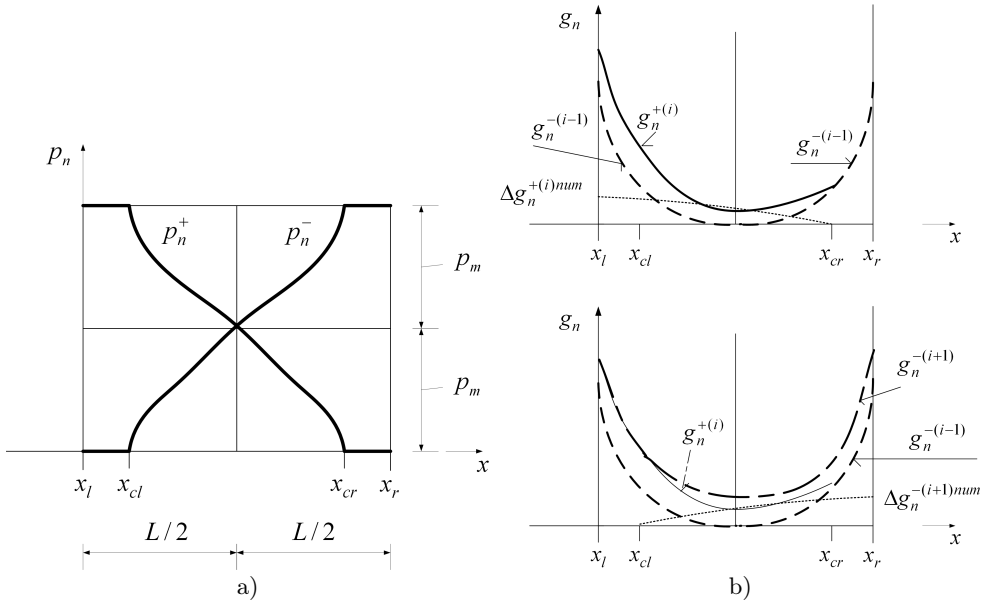


Figure 23. Contact pressure distribution and shape evolution. a) $p_n$ at steady state, b) shape modification in the $i$-th (+ direction sliding) and $(i+1)$-th (- direction sliding) iterational step

.

If $\Delta p_n \neq 0$ the shape must be changed, that is instead of (50) it can be written

$$\Delta p_n^{\pm} = p_n^+ + p_n^- - 2p_m = c_n(u_n^+ + g_n^{\mp} + u_n^- + g_n^{\pm}) + c\Delta g_n^{\pm} - 2p_m \tag{51}$$

The optimization problem can be written in the following form

$$\min_{g_n}\{\int_{S_c} \frac{1}{2}(p_n^+ + p_n^- - 2p_m)^2 \,\mathrm{d}S \mid p_n^{\pm} \geqslant 0,\ \ d_n^{\pm} \geqslant 0,\ \ p_n^{\pm}\, d_n^{\pm} = 0,$$

$$\tau_n^+ = \mu\, p_n^+,\ \ \tau_n^- = -\mu\, p_n^-,\ \ \text{Equilibrium equations for punch}\} \tag{52}$$

where the minimum of (52) provides the contact pressure distribution satisfying (49) if $\Delta p_n = 0$. The shear stress $\tau_n^{\pm}$ acts on the contact surface of Body 1 in the direction of $x$-axis.

For solution of the minimization problem (52) a special iterational process is recommended. In each step the Signorini contact conditions $p_n^{\pm}\, d_n^{\pm} = 0$, $p_n^{\pm} \geq 0$, $d_n^{\pm} \geq 0$ and the Coulomb dry friction law $\tau_n^+ = \mu p_n^+$, $\tau_n^- = -\mu p_n^-$ must be satisfied in the solution of the contact problem and next the modified contact shape should be determined. The shape modification is taken from equation (51).

Consider the half cycle $i$ of the + sliding direction, next $i+1$ of the – sliding direction and similarly the consecutive half cycle $i+2$ for + sliding direction and $i+3$ for – direction of sliding and so on.

According to Figure 23 in the interval $x_l \le x \le x_{cl}$ the contact pressures are $0 \le p_n^+$, $p_n^- = 0$ in the interval $x_{cl} \le x \le x_{cr}$ the pressures are $0 \le p_n^+$, $0 \le p_n^-$ and in the interval $x_{cr} \le x \le x_r$ the pressures are $p_n^+ = 0$, $0 \le p_n^-$.

Let us begin the $i$-th half cycle. Then

$$\Delta p_n^{\pm} = p_n^+ + p_n^- - 2p_m = c_n(u_n^+ + g_n^{\mp} + u_n^- + g_n^{\pm}) + c\Delta g_n^{\pm} - 2p_m \tag{53}$$

in the interval $x_l \le x \le x_{cl}$ because $g_n^{+(i)} = g_n^{-(i-1)} + \Delta g_n^{+(i)}$. It is supposed that in the right direction of sliding at the end of half cycle the new shape is modified by $\Delta g_n^{+(i)}$. The modification of the shape is

$$\frac{\Delta p_n^+}{c_n} - (u_n^{+(i)} + g_n^{-(i-1)}) = \Delta g_n^{+(i)} - \frac{2p_m}{c_n} = \Delta \tilde{g}_n^{+(i)} \,. \tag{54}$$

In the interval $x_{cl} \le x \le x_{cr}$ in right direction

$$\Delta p_n^+ = p_n^{+(i)} + p_n^{-(i-1)} - 2p_m = \\ = c_n(u_n^{+(i)} + g_n^{-(i-1)} + u_n^{-(i-1)} + g_n^{-(i-1)}) + c_n\Delta g_n^{+(i)} - 2p_m \,, \tag{55}$$

$$\frac{\Delta p_n^+}{c_n} - (u_n^{+(i)} + u_n^{-(i-1)} + 2g_n^{(i-1)}) = \Delta g_n^{+(i)} - \frac{2p_m}{c_n} = \Delta \tilde{g}_n^{+(i)} \,. \tag{56}$$

For numerical calculation it is supposed that at the point $x_{cr}$ of the contact domain the modification of the gap is equal to zero, that is $\Delta \tilde{g}_n^{+(i)} - \Delta \tilde{g}_n^{+(i)}(x_{cr}) = \Delta g_n^{+(i)\,num}$ and the new shape at the end of + direction motion is

$$g_n^{+(i)} = g_n^{-(i-1)} + \Delta g_n^{+(i)\,num} \,. \tag{57}$$

In the interval $x_{cr} \le x \le x_r$ in the left direction we have

$$\Delta p_n^- = p_n^{-(i+1)} - 2p_m = c_n(u_n^{-(i+1)} + g_n^{+(i)}) + c_n\Delta g_n^{-(i+1)} - 2p_m \tag{58}$$

that is

$$\frac{\Delta p_n^-}{c_n} - (u_n^{-(i+1)} + g_n^{+(i)}) = \Delta g_n^{-(i+1)} - \frac{2p_m}{c_n} = \Delta \tilde{g}_n^{-(i+1)} \tag{59}$$

and in the interval $x_{cl} \le x \le x_{cr}$ for the left direction there is

$$\Delta p_n^- = p_n^{+(i)} + p_n^{-(i+1)} - 2p_m = \\ = c_n(u_n^{+(i)} + (g_n^{-(i-1)} + \Delta g_n^{+(i)}) + u_n^{-(i+1)} + g_n^{+(i)}) + c_n\Delta g_n^{-(i+1)} - 2p_m$$

where $g_n^{+(i)} = g_n^{-(i+1)} + \Delta g_n^{+(i)}$, thus

$$\Delta p_n^- = p_n^{+(i)} + p_n^{-(i+1)} - 2p_m = c_n(u_n^{+(i)} + u_n^{-(i+1)} + 2g_n^{+(i)}) + c_c\Delta g_n^{-(i+1)} - 2p_m \tag{60}$$

and

$$\frac{\Delta p_n^-}{c_n} - (u_n^{+(i)} + u_n^{-(i+1)} + 2g_n^{+(i)}) = \Delta g_n^{-(i+1)} - \frac{2p_m}{c_n} = \Delta \tilde{g}_n^{-(i+1)} \,. \tag{61}$$

Since in point $x_{cl}$ the modification of the gap is equal to zero

$$\Delta \tilde{g}_n^{-(i+1)} - \Delta \tilde{g}_n^{-(i+1)}(x_{cl}) = \Delta g_n^{-(i+1)\,num}$$

for numerical calculation the modification of the gap will be

$$g_n^{-(i+1)} = g_n^{+(i)} + \Delta g_n^{-(i+1)\,num} \tag{62}$$

Now repeat the calculations for the consecutive period
Right motion:

$$x_l \le x \le x_{cl} \quad \frac{\Delta p_n^+}{c_n} - (u_n^{+(i+2)} + g_n^{-(i+1)}) = \Delta g_n^{+(i+2)} - \frac{2p_m}{c_n} = \Delta \tilde{g}_n^{+(i+2)} \tag{63}$$

$$\begin{aligned} x_{cl} \le x \le x_{cr} \quad & \frac{\Delta p_n^+}{c_n} - (u_n^{+(i+2)} + g_n^{-(i+1)} + u_n^{-(i+1)} + g_n^{-(i+1)}) = \Delta g_n^{+(i+2)} - \frac{2p_m}{c_n} \\ & \frac{\Delta p_n^+}{c_n} - (u_n^{+(i+2)} + u_n^{-(i+1)} + 2g_n^{-(i+1)}) = \Delta g_n^{+(i+2)} - \frac{2p_m}{c_n} = \Delta \tilde{g}_n^{+(i+2)} \end{aligned} \tag{64}$$

Left motion

$$x_{cr} \le x \le x_r \quad \frac{\Delta p_n^-}{c_n} - (u_n^{-(i+3)} + g_n^{+(i+2)}) = \Delta g_n^{-(i+3)} - \frac{2p_m}{c_n} = \Delta \tilde{g}_n^{-(i+3)} \tag{65}$$

$$\begin{aligned} x_{cl} \le x \le x_{cr} \quad & \frac{\Delta p_n^-}{c_n} - (u_n^{+(i+2)} + g_n^{+(i+2)} + u_n^{-(i+3)} + g_n^{+(i+2)}) = \Delta g_n^{-(i+3)} - \frac{2p_m}{c_n} \\ & \frac{\Delta p_n^-}{c_n} - (u_n^{+(i+2)} + u_n^{-(i+3)} + 2g_n^{+(i+2)}) = \Delta g_n^{-(i+3)} - \frac{2p_m}{c_n} = \Delta \tilde{g}_n^{-(i+3)} \end{aligned} \tag{66}$$

where

$$\Delta \tilde{g}_n^{+(i+2)} - \Delta \tilde{g}_n^{+(i+2)}(x_{cr}) = \Delta g_n^{+(i+2)\,num}, \qquad g_n^{+(i+2)} = g_n^{-(i+1)} + \Delta g_n^{+(i+2)\,num},$$
$$\Delta \tilde{g}_n^{-(i+3)} - \Delta \tilde{g}_n^{-(i+3)}(x_{cl}) = \Delta g_n^{-(i+3)\,num}, \qquad g_n^{-(i+3)} = g_n^{+(i+2)} + \Delta g_n^{-(i+3)\,num}.$$

In this formulation for one period and (i+2-i+3) -th steps, the change of the shape is

$$g_n^{-(i+3)} = g_n^{-(i+1)} + \Delta g_n^{+(i+2)\,num} + \Delta g_n^{-(i+3)\,num} \tag{67}$$

In the numerical calculation for each cycle, initially the shape at the point $x = 0.5(x_l + x_r)$, $z = 100$ is set to zero value, that is the shape is moved vertically to this point.

**Example 1:**
For determination of the shape in periodic steady state for the punch Figure 2a, let us apply the above iteration process. The initial shape is taken from the solution for averaged monotonic sliding. Using this initial form the proposed iteration procedure must be performed for approximately 500 iteration steps. The shape evolution is shown in Figure 24a. At the beginning the contact pressure has a high value at the borders of contact domain (see Figure 24b). After ∼300 steps the shape is close to the steady periodic shape form (see Figure24a). In prectice after 500 steps the iterative procedure provides accurate prediction – see Figure 24d.

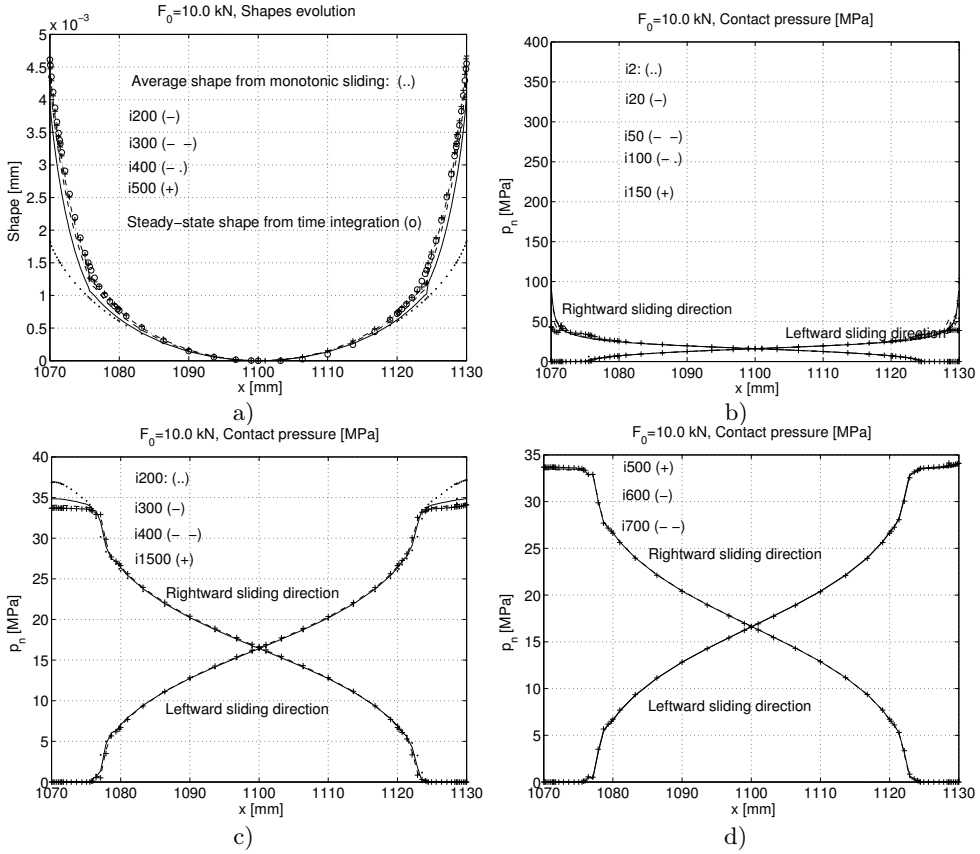


Figure 24. Determination of the shape for steady state periodic motion for the construction in Figure 19. a) Evolution of the shape in the iteration process, b)-d) evolution of the contact pressure.

**Example 2:**
In this example the punch constraint of Figure 2a is modified. The support is only placed at one point / pin at point ($x = 1030, z = 140$) – see Figure 2b. The initial shape is also taken from the result for averaged monotonic sliding, see Figure 25c with curve (...). To reach the steady state, approximately 300 iteration steps should be executed. Initially the contact pressure has a high value at the borders of contact domain. Figure 25e presents the sum of contact pressures, which has a high value at the borders of contact zone in the beginning stage of the wear process. In the steady periodic state this sum is close to the $2p_m = 33.333$ MPa. After 200 steps the shape is close to the steady shape form (Figure 25d). We remark that after 300 steps the distribution of contact pressure does not change – see Figure 25b. The solution of the optimization problem (52) by penalty technique is characterized by the slow convergence, but the form of the contact shape can be determined with high accuracy.

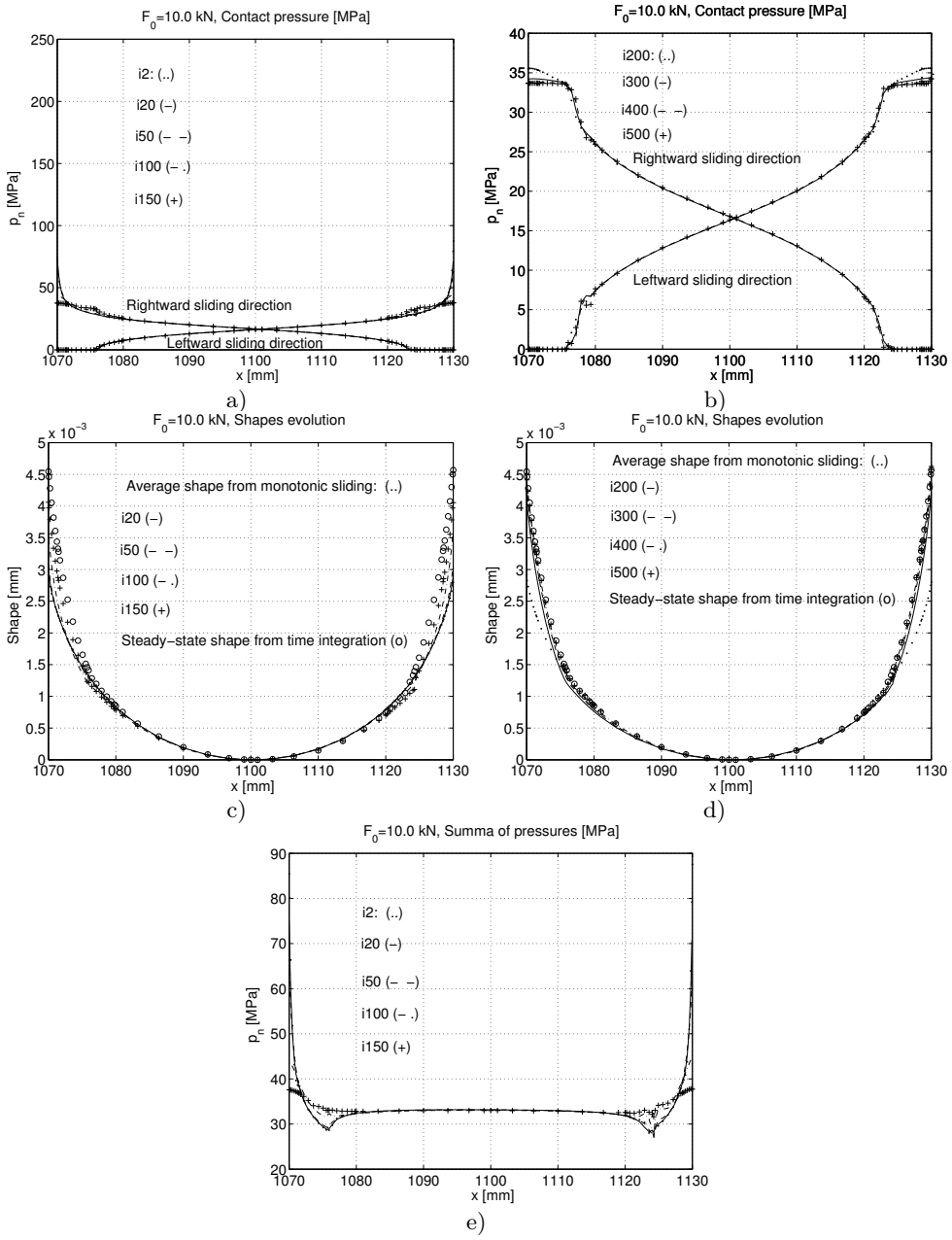


Figure 25. Optimization result for a plane punch with support at $l_z = 40$ mm. a) evolution of the contact pressure, b) contact pressure distribution near the steady state, c), d) evolution of the shape in the iteration process, e) evolution of the sum of contact pressures in the iteration process.

## 7. Conclusion

In our analysis the relative contact sliding displacements were considered and the partial slip displacements were neglected. The relative periodic sliding motion between contacting bodies induces a periodic steady wear state with different distributions of contact pressure during the leftward and rightward sliding directions. These pressure distributions cannot be specified from minimization of the wear dissipation in one sliding period. They are determined by solving the boundary value problem with imposed periodicity and contact compatibility conditions. On the other hand, the summed $p_\Sigma$ contact pressure value for consecutive semi-cycles results from rigid body wear displacement of the punch. In the steady periodic wear state the wear dissipation during one cycle reaches its minimum and specifies the summed contact pressure. The specific examples presented in the paper illustrate the solution method for periodic wear states.

By solving the optimization problem (41) or (53), we can generate the shape and the contact pressure distributions with high accuracy without time integration of the wear rule for periodic sliding. The results of steady states for monotonic sliding provide fairly good simple predictions for shapes generated in the steady periodic wear states

## Appendix A. Periodic sliding along a cylindrical contact surface

Consider a 2D contact problem for fixed loads and periodically varying relative sliding velocity between two bodies interacting on a cylindrical contact surface as in Figure 26. Body 1 (punch) is allowed to translate vertically in $z$-direction and rotate around $y$-axis located at point O. Body 2 (substrate) is a circular disc of radius $R_0$ executing periodic rotation through the angle $[+\alpha, -\alpha]$ with the relative velocity $\dot{u}_\tau$, $v_r = \|\dot{\boldsymbol{u}}_\tau\|$. The wear rate in normal contact direction is specified by the rule

$$\dot{w}_{i,n} = \beta_i v_r^{a_i} p_n^{b_i} \qquad i = 1, 2\,. \tag{A.1}$$

It is assumed that during the steady periodic state the wear increment accumulated during one cycle should be compatible at each point $x \in S_c$ with the rigid body punch motion. Assume the rigid body wear velocities for left (-) and right (+) sliding directions of the substrate in the following form

$$\dot{\lambda}_F^- = -\dot{\lambda}_F^- \boldsymbol{e}_z\,, \quad \dot{\lambda}_M^- = -\dot{\lambda}_M^- \boldsymbol{e}_y\,, \qquad \dot{\lambda}_F^+ = -\dot{\lambda}_F^+ \boldsymbol{e}_z\,, \quad \dot{\lambda}_M^+ = \dot{\lambda}_M^+ \boldsymbol{e}_y\,. \tag{A.2}$$

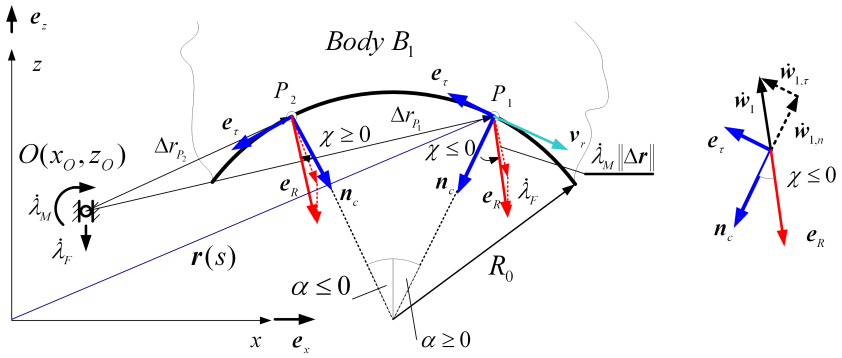


Figure 26. Body 1 can move as a rigid body in vertical direction and rotate around O. The wear velocity is not normal to the contact surface. Its direction $\boldsymbol{e}_R$ is defined by the rigid body velocities $\dot{\boldsymbol{\lambda}}_F^{\pm}$, $\dot{\boldsymbol{\lambda}}_M^{\pm}$ according to (A.4).

Thus the velocities at an arbitrary point at the punch are

$$\dot{\boldsymbol{w}}_R^+ = \dot{\boldsymbol{\lambda}}_F^+ + \dot{\boldsymbol{\lambda}}_M^+ \times \boldsymbol{r}_{OP}\,, \quad \dot{\boldsymbol{w}}_R^- = \dot{\boldsymbol{\lambda}}_F^- + \dot{\boldsymbol{\lambda}}_M^- \times \boldsymbol{r}_{OP} \tag{A.3}$$

and the summed wear velocity for consecutive semi-cycles is

$$\dot{\boldsymbol{w}}_R = (\dot{\boldsymbol{\lambda}}_F^+ + \dot{\boldsymbol{\lambda}}_F^-) + (\dot{\boldsymbol{\lambda}}_M^+ + \dot{\boldsymbol{\lambda}}_M^-) \times \boldsymbol{r}_{OP} = -(\dot{\lambda}_F^+ + \dot{\lambda}_F^-)\, \boldsymbol{e}_z + (\dot{\lambda}_M^+ - \dot{\lambda}_M^-)\, \boldsymbol{e}_y \times \boldsymbol{r}_{OP} \tag{A.4}$$

The displacement resulting from this velocity equals

$$\Delta \boldsymbol{w}_R = -(\Delta\lambda_F^+ + \Delta\boldsymbol{\lambda}_F^-)\, \boldsymbol{e}_z + (\Delta\lambda_M^+ - \Delta\lambda_M^-)\, \boldsymbol{e}_y \times \boldsymbol{r}_{OP} = -\Delta\lambda_F\, \boldsymbol{e}_z + \Delta\lambda_M\, \boldsymbol{e}_y \times \boldsymbol{r}_{OP} \tag{A.5}$$

where

$$\Delta\lambda_{F,M}^+ = \int_0^{T_*/2} \dot{\lambda}_{F,M}^+ dt, \qquad \Delta\lambda_{F,M}^- \int_{T_*/2}^{T_*} \dot{\lambda}_{F,M}^- dt\,.$$

The normal and tangential unit vector components are

$$\boldsymbol{n}_c = -\cos\alpha\, \boldsymbol{e}_z - \sin\alpha\, \boldsymbol{e}_x\,, \quad \boldsymbol{e}_\tau = \sin\alpha\, \boldsymbol{e}_z - \cos\alpha\, \boldsymbol{e}_x\,. \tag{A.6}$$

Thus, the total wear in normal direction accumulated during one sliding cycle is

$$\Delta w_n = \Delta \boldsymbol{w}_R \cdot \boldsymbol{n}_c = \Delta\lambda_F\, \cos\alpha + \Delta\lambda_M\, [(x_P - x_O)\cos\alpha - (z_P - z_O)\sin\alpha] \tag{A.7}$$

The wear velocity vector for two bodies is coaxial with rigid body wear velocity, that is

$$\dot{\boldsymbol{w}}_R = \dot{\boldsymbol{w}}_2 - \dot{\boldsymbol{w}}_1\,. \tag{A.8}$$

Assuming $\tilde{\beta}_1 \neq 0$, $\tilde{\beta}_2 = 0$ (the material is removed only from Body 1), the wear velocity of Body 1 on the contact surface is expressed in the form

$$\dot{\boldsymbol{w}}_R = -\dot{\boldsymbol{w}}_1 = -(-\dot{w}_{1,n}\, \boldsymbol{n}_c + w_{1,\tau}\, \boldsymbol{e}_\tau)\,, \quad \dot{w}_n = \dot{\boldsymbol{w}}_R \cdot \boldsymbol{n}_c = -\dot{\boldsymbol{w}}_1 \cdot \boldsymbol{n}_c = \dot{w}_{1,n} \tag{A.9}$$

and its increment for one sliding period is

$$\Delta w_n = \Delta \boldsymbol{w}_R \cdot \boldsymbol{n}_c = -\Delta \boldsymbol{w}_1 \cdot \boldsymbol{n}_c = \Delta w_{1,n}\,. \tag{A.10}$$

In this way, the wear increment in normal direction can be calculated easily, thus

$$\Delta w_{1,n} = -\Delta \boldsymbol{w}_1 \cdot \boldsymbol{n}_c = \Delta\lambda_F \cos\alpha + \Delta\lambda_M \left[(x_P - x_O)\cos\alpha - (z_P - z_O)\sin\alpha\right] . \tag{A.11}$$

This value of wear can also be calculated from the wear rule, assuming $a_1 = b_1 = 1$, thus

$$\Delta w_{1,n} = \Delta w_{1,n}^{+} + \Delta w_{1,n}^{-} = \tilde{\beta}_1 \int_0^{T_*/2} \|\dot{\boldsymbol{u}}_\tau\| \; p_n^{+} dt \; + \tilde{\beta}_1 \int_{T_*/2}^{T_*} \|\dot{\boldsymbol{u}}_\tau\| \; p_n^{-} dt$$

$$\Delta w_{1,n} = \Delta w_{1,n}^{+} + \Delta w_{1,n}^{-} = \tilde{\beta}_1 \int_0^{T_*/2} \|\dot{\boldsymbol{u}}_\tau\| \; dt \;\; (p_n^{+} + p_n^{-}) = Q \; (p_n^{+} + p_n^{-}) = Q \; 2p_m = Q \, p_\Sigma \tag{A.12}$$

where

$$p_m = (p_n^{+} + p_n^{-})/2 = p_\Sigma/2 \,, \quad Q = \tilde{\beta}_1 \int_0^{T_*/2} \|\dot{\boldsymbol{u}}_\tau\| \; dt \,.$$

Comparing (A.11) and (A.12), it is seen that the distribution of the sum of contact pressure values of consecutive semi-cycles can be expressed as a function of position, thus

$$p_\Sigma/2 = p_m = p_m^C \cos\alpha + p_m^L \left[(x_P - x_O)\cos\alpha - (z_P - z_O)\sin\alpha\right] \tag{A.13}$$

that is

$$\begin{aligned} \Delta w_{1,n} &= \Delta\lambda_F \cos\alpha + \Delta\lambda_M \left[(x_P - x_O)\cos\alpha - (z_P - z_O)\sin\alpha\right] = \\ &= \tilde{\beta}_1 \int_0^{T_*/2} \|\dot{\boldsymbol{u}}_\tau\| \; dt \; 2 \left\{ p_m^C \cos\alpha + p_m^L \left[(x_P - x_O)\cos\alpha - (z_P - z_O)\sin\alpha\right] \right\} \end{aligned}$$

where $\Delta\lambda_{F,M}^{\pm}$ is the increment of rigid body wear velocities in the half period time, $p_m^C$, $p_m^L$ are unknowns, which can be calculated from equilibrium equations.

The punch is assumed to be loaded by the resultant vertical load $F_0$ and the moment $M_0$ relative to the support point $O$. Using the equilibrium equations for summed loads, it can be written

$$0 = 2\boldsymbol{f}_0 + \int_{S_c} (\boldsymbol{t}^{c+} + \boldsymbol{t}^{c-}) \, dS \tag{A.14a}$$

$$0 = 2\boldsymbol{m}_0 + \int_{S_c} \boldsymbol{r}_{OP} \times (\boldsymbol{t}^{c+} + \boldsymbol{t}^{c-}) \, dS \tag{A.14b}$$

where

$$\boldsymbol{t}^{c+} = -p_n^{+} \boldsymbol{n}_c - \mu \, p_n^{+} \boldsymbol{e}_\tau \,, \quad \boldsymbol{t}^{c-} = -p_n^{-} \boldsymbol{n}_c + \mu \, p_n^{-} \boldsymbol{e}_\tau \,,$$

$S_c$ is the area of contact zone, $\boldsymbol{f}_0 = -F_0\boldsymbol{e}_z$, $\boldsymbol{m}_0 = M_0\boldsymbol{e}_y$ resultant force and moment, respectively, of the specified loading. The projection of (A.14a) on $\boldsymbol{e}_z$ gives

$$0 = -2F_0 + \boldsymbol{e}_z \cdot \int\limits_{S_c} (\boldsymbol{t}^{c+} + \boldsymbol{t}^{c-})\, dS =$$

$$= -2F_0 + \int\limits_{S_c} \{\ (p_n^+ + p_n^-)\ \cos\alpha - \mu\,(p_n^+ - p_n^-)\sin\alpha\ \}\ \ t_{th}\, R_0\, d\alpha$$

or

$$0 = -2F_0 + \int\limits_{S_c} \{\ 2p_m \cos\alpha - \mu\,(p_n^+ - p_n^-)\sin\alpha\ \}\ \ t_{th}\, R_0\, d\alpha\,. \tag{A.15}$$

The moment equilibrium equation has the form

$$0 = 2\boldsymbol{m}_0 \cdot \boldsymbol{e}_y + \boldsymbol{e}_y \cdot \int\limits_{S_c} \boldsymbol{r}_{OP} \times (\boldsymbol{t}^{c+} + \boldsymbol{t}^{c-})\, dS =$$

$$= 2M_0 - \int\limits_{Sc} 2p_m\, [(z_P - z_O)\ \sin\alpha - (x_P - x_O)\ \cos\alpha]\ \ t_{th}\, R_0\, d\alpha +$$

$$+ \int\limits_{S_c} \mu(p_n^+ - p_n^-)\ [(z_P - z_O)\ \cos\alpha + (x_P - x_O)\ \sin\alpha]\ \ t_{th}\, R_0\, d\alpha \tag{A.16}$$

where $t_{th}$ is the disc and punch thickness.

We have two equations for calculation of $p_m^C$ and $p_m^L$ occurring in (A.13). For some cases we find a direct way to calculate these parameters.

Some remarks:

1. If $\dot{\lambda}_M = 0$, then $p_m = p_m^C \cos\alpha$ and in this case from (A.15) we find
$$p_m^C = F_0 / \int\limits_{S_c} (\cos\alpha)^2\, t_{th} R_0 d\alpha$$
2. If the contact surface is plane ($\alpha = 0$), then from (A.13) we have $p_m = p_m^C + p_m^L(x_P - x_O)$. The values of $p_m^C$and $p_m^L$ can be calculated from (A.15) and (A.16): Using $dS = t_{th}R_0\, d\alpha$ and $\Delta z = z_P - z_O = const$ we get $\int\limits_{S_c} \mu(p_n^+ - p_n^-)\Delta z dS = 0$ since
$$\mu \int\limits_{S_c} (p_n^+ - p_n^-)\Delta z dS = \Delta z \mu (\int\limits_{S_c} p_n^+ dS - \int\limits_{S_c} p_n^- dS) = \Delta z(\mu F_0 - \mu F_0) = 0\,.$$
Consequently the moment of the shear contact stress is equal to zero.
3. If in the integrals (A.15) and (A.16) the terms$\mu(p_n^+ - p_n^-)$ are negligible, then $p_m^C$ and $p_m^L$ can be calculated and can be regarded as the first approximations of exact values.

Assume the relative tangential displacement on the contact surface in the form $\boldsymbol{u}_\tau = u_0 \cos\omega t \boldsymbol{e}_\tau$ Then the relative velocity is $v_r = \|\dot{\boldsymbol{u}}_\tau\| = \omega u_0 \sin \omega t$.

The wear increment in one period (note that the contact pressure is fixed in half period) equals

$$\Delta w_{1,n} = \tilde{\beta}_1 \left[p_n^+ + p_n^-\right] (u_0\omega) \int_0^{T_*/2} |\sin \omega\tau| \, \mathrm{d}\tau \tag{A.17}$$

which, using the equalities $\int_0^{T_*/2} v_r \mathrm{d}\tau = \int_{T_*/2}^{T_*} v_r \mathrm{d}\tau = 2u_0$, provides the simple relation

$$\Delta w_{1,n} = \tilde{\beta}_1 \left[p_n^+ + p_n^-\right] \, 2u_0 = Q \, p_\Sigma \tag{A.18}$$

where $Q = \tilde{\beta}_1 \, 2u_0$.

The averaged wear rate in one period equals

$$\overline{\dot{w}}_{1,n} = \frac{\Delta w_{1,n}}{T_*} = \frac{\tilde{\beta}_1[p_n^+ + p_n^-]}{T_*} 2u_0 = \frac{Q \, p_\Sigma}{T_*} \tag{A.19}$$

If the rigid body wear velocity $\dot{\lambda}_M^+ = \dot{\lambda}_M^- = 0$, then $\dot{\lambda}_F^+ \neq 0$, $\dot{\lambda}_F^- \neq 0$, $p_m = p_m^C \cos\alpha$, $p_\Sigma = 2p_m = 2p_m^C \cos\alpha$ and

$$\Delta w_R = \frac{\Delta w_{1,n}}{\cos\alpha} = \frac{Q \, p_\Sigma}{\cos\alpha} = Q \, 2p_m^C = const \tag{A.20}$$

that is in the steady periodic wear regime the uniform vertical (rigid body) wear increment is accumulated during the full cycle at each point of the contact zone.

**Acknowledgements.** The present research was partially supported by the Hungarian Academy of Sciences, grants OTKA K67825 National Research, and Development and Innovation Office - NKFIH, K115701, and by projects TÁMOP-4.2.1.B-10/2/KONV-2010-0001 and TÁMOP-4.2.2/B-10/1-2010-0008.

## REFERENCES

1. Páczelt, I. and Mróz, Z.: On the analysis of steady sliding wear process. *Tribology International*, **42**, (2009), 275–283.
2. Páczelt, I. and Mróz, Z.: Variational approach to the analysis of steady state thermo-elastic wear regimes. *Int. J. Num. Meth. Eng.*, **81**, (2010), 728–760.
3. Mróz, Z. and Páczelt, I.: Analysis of thermo-elastic wear problems. *J. Thermal Stresses*, **34-35**, (2011), 569–606.
4. Páczelt, I. and Mróz, Z.: Numerical analysis of steady thermo-elastic wear regimes induced by translating and rotating punches. *Computers and Structures*, **89**, (2011), 2495–2521.
5. Goryacheva, I. G., Rajeev, P. T., and Farris, T. N.: Wear in partial slip contact. *J. Tribology*, **123**, (2001), 848–856.
6. McColl, I. R., Ding, J., and Leen, S. B.: Finite element simulation and experimental validation of fretting wear. *Wear*, **256**, (2004), 1114–1127.

7. Ding, J., Leen, S. B., and McColl, I. R.: The effect of slip regime on fretting wear-induced stress evolution. *Int. J. Fatigue*, **26**, (2004), 521–531.

8. Fouvry, S., Paulin, C., and Liskiewicz, T.: Application of an energy wear approach to quantify fretting contact durability: introduction of a wear energy capacity concept. *Tribology International*, **40**, (2007), 1428–1440.

9. Fouvry, S., Liskiewicz, T., and Paulin, C.: A global-local wear approach to quantify the contact endurance under reciprocating-fretting sliding conditions. *Wear*, **263**, (2007), 518–531.

10. Peigney, U.: Simulating wear under cyclic loading by a minimization approach. *Int. J. Solids Struct.*, **41**, (2004), 6783–6799.

11. Kim, N. H., Won, D., Burris, D., Holtkamp, B., Gessel, G. C., Swanson, P., and Sawyer, W. G.: Finite element analysis and experiments of metal/metal wear in oscillatory contacts. *Wear*, **258**, (2005), 1787–1793.

12. Páczelt, I. and Mróz, Z.: On steady wear states for monotonic relative sliding of contacting bodies. *Key Engineering Materials*, **618**, (2014), 49–71.

13. Páczelt, I. and Mróz, Z.: Solution of wear problems for monotonic and periodic sliding with p-version of the finite element method. *Comput. Methods Appl. Mech. Engng.*, **249-252**, (2012), 75–103.

14. Szabó, B. and Babuska, I.: *Finite Element Aanalysis*. Wiley Intersience, New York, 1991.

15. Páczelt, I. and Mróz, Z.: Analysis of thermo-mechanical wear problems for reciprocal punch sliding. *Advances in Engineering Software*, **80**, (2015), 139–155.

16. Zavarise, G., Wriggers, P., and Schrefler, B.: On augmented lagrangian algorithms for thermomechanical contact problems with friction. *Int. J. Num. Meth. Eng.*, **38**, (1995), 2929–2949.

17. Páczelt, I., Szabó, B., and Szabó, T.: Solution of contact problem using the hp-version of the finite element method. *Comput. Math. Appl.*, **38**, (2000), 49–69.

18. Ou, H., Lu, B., Cui, Z. S., and Lin, C.: A direct shape optimization approach for contact problems with boundary stress concentration. *Journal of Mechanical Science and Technology*, **27**(9), (2013), 2751–2759.